AIMS Mathematics, 10(4): 8827–8872.
DOI: 10.3934/math.2025405
Received: 14 January 2025
Revised: 04 April 2025
Accepted: 08 April 2025
Published: 17 April 2025

https://www.aimspress.com/journal/Math

Research article

Dynamics of a fractal-fractional mathematical model for the management of waste plastic in the ocean with four different numerical approaches

Chatthai Thaiprayoon[1], Jutarat Kongson[1] and Weerawat Sudsutad[2,*]

[1] Research Group of Theoretical and Computational Applied Science, Department of Mathematics, Faculty of Science, Burapha University, Chonburi 20131, Thailand

[2] Department of Statistics, Faculty of Science, Ramkhamhaeng University, Bangkok 10240, Thailand

* **Correspondence:** Email: weerawat.s@rumail.ru.ac.th.

Abstract: This work studies a fractional model in the context of the fractal-fractional operator involving a power law kernel for waste plastic in the ocean consisting of waste plastic material, marine debris, and reprocessing. The novelty of this study lies in utilizing the fractal-fractional framework to analyze the behavior of the proposed model and derive qualitative theoretical results. We investigated the equilibrium points and analyzed their stability using the basic reproduction number. We examined the global stability of possible equilibrium points, as well as their unstable conditions. The sensitivity analysis can also help to better understand the model's dynamics better. The existence and uniqueness of results were studied by utilizing Banach's contraction mapping principle, while Ulam's stability for the proposed model was also investigated. Furthermore, we derived the numerical algorithms by utilizing four different techniques, including the decomposition, Adams-Bashforth, Newton polynomial, and predictor-corrector methods. By providing the input factor values, we illustrated the graphic numerical simulations to enhance our understanding of the waste plastic process and optimize the control strategies. Moreover, we compare ordinary, fractional, and fractal-fractional derivatives in the sense of the Caputo type with the reported real data of 70 years.

Keywords: waste plastic management; Volterra-type Lyapunov function; fractal-fractional derivative; Ulam-Hyers stability; numerical scheme
Mathematics Subject Classification: 34A08, 34A34, 34D20, 65L05

1. Introduction

Marine debris is currently a major environmental concern. It consists of human-made waste that has been purposefully or unintentionally dumped into oceans, rivers, and other vast bodies of water. There are many types of marine debris, but the most common type is plastic. Plastic is now

widely used in everyday objects like plastic bags, water bottles, and food containers and in large-scale industries like consumer goods production and the electronics and automotive industries. It is made from chemical compounds known as polymers, synthesized by chemicals primarily derived from petroleum and natural gas. Its advantages include being lightweight, durable, water-resistant, hygienic, cheap producing cost, and versatile in its applications. Plastic containers and products significantly impact both environmental productivity and worldwide economic growth. However, even though plastics offer numerous advantages, the ecological impact and the need for responsible use must also be considered. Due to the large amount of plastic manufactured, as well as its durability and resistance to degradation, plastic has become a serious environmental issue, resulting in plastic waste in the environment, particularly in the ocean. When plastic garbage is not suitably handled, it can have severe consequences for ecosystems, sea animals, and human health. Plastic disposal and degradation are lengthy processes influenced by various factors, including the type of plastic and environmental conditions. Many countries have programs to limit plastic use, including developing plastic reusable technologies. Recycling plastic is one key potential solution for reducing waste plastic. It involves several key steps to transform discarded plastic items into new products.

Mathematical models are popularly utilized in the areas of natural sciences, engineering, and social science to simulate natural phenomena in real-world problems. Many researchers are interested in topics where plastic waste problems are being modeled with the goal of reducing the large amounts of garbage in the environment, a mounting crisis. With the help of mathematical models, researchers can better comprehend and address the complicated issue of waste plastic, resulting in more effective solutions and sustainable practices. Some works of literature on the waste plastic issue have been studied and published, such as Nuwairan et al. [1] who applied an artificial neural network method and the Levenberg-Marquardt backpropagation characteristic to study the nonlinear mathematical form for the management of waste plastic on the ocean (WPO) surface. Chaturvedi et al. [2] used mathematical modeling to analyze the pollution of plastic waste and its effect on the ocean system. To anticipate yearly plastic production volume and waste generation, Addor et al. [3] created a basic cyclical dynamic closed model that reflects the whole plastic life cycle. Their works used the Laplace transform technique as the solution methodology and predicted the values of global plastic yearly production and waste generation by specialized techniques. Lzadi et al. [4] investigated and studied the model of an ocean waste plastic management system.

Fractional calculus is a field of mathematical analysis that differs from and builds on the capabilities of traditional calculus. It generalizes the ideas of differentiation and integration to arbitrary orders, whereas traditional calculus deals with integer orders. With the restriction of integer-order operations, the analysis of mathematical models utilizing fractional derivatives rather than traditional derivatives yields more realistic and meaningful insights that are easier to comprehend because it allows any rational number as an order. Fractional derivatives give a powerful instrument for simulating and analyzing systems with memory and hereditary properties. It can describe heredity phenomena in the dynamical system, making it popularly applicable in various domains, including mathematics, physics, engineering, biology, medicine, and finance. Several fractional operators have been invented, each with unique properties and applications, such as Riemann-Liouville (RL), Caputo, Hadamard, Caputo-Fabrizio, Katugampola, Hilfer, and (k,ψ)-Hilfer proportional [5–10]. Recently, Atangana [11] introduced the concept of fractal-fractional (FF) operators, which integrate principles from both fractional and fractal calculus. These operators can be formulated using various kernel functions,

including the power law, the exponential law, and the Mittag-Leffler function. A key feature of fractal-fractional order differential equations is their ability to transform both the order and the dimension of a system into arbitrary rational values, thereby providing a more comprehensive framework for modeling complex real-world phenomena. The role of fractional operators has incredibly impactful real-world applications in many fields, such as engineering, biology, physics, and medicine. For various examples of fractional calculus applications with different areas of study, the reader may refer to [12–15] and its references. Moreover, according to the review of several articles on waste plastic in the ocean, there is not much direct research on this topic corresponding with fractional-order operators. Here, we introduce some related works: Nuwairan et al. [16] studied numerical investigation for a fractional order in the sense of RL of the management of waste plastic in the ocean. Joshi et al. [17] studied a model under the Caputo fractional derivative operator for the plastic waste model to understand the effect of burned plastic and reused plastic on air pollution. Priya and Sabarmathi [18] applied the Atangana-Baleanu-Caputo derivative operator for the model of micro-plastic pollution in soil and its impact on the nutrient cycle. Parsamanesh and Izadi [19] established the global stability and bifurcations in a model for the WPO model. Ulam stability is an efficient tool for offering insights into the strength of mathematical models. It ensures the existence of an exact solution close to the approximate one in cases where finding exact solutions may be computationally complicated or infeasible. Ulam's stability originated in 1940 by a mathematician named Ulam and was later developed by Hyers in 1941 and extended by Rassias in 1978 [20–22]. Ulam stability is currently classified into numerous forms, including Ulam-Hyers (UH) stability, Ulam-Hyers-Rassias (UHR) stability, generalized UH (GUH) stability, generalized UHR (GUHR) stability, and others.

Inspired by the above discussion, this study aims to employ the FFP operator with a power-law kernel to effectively capture the memory and hereditary characteristics inherent in fractional-order differential equations. These properties are crucial for modeling complex system behaviors, particularly in the context of plastic waste and recycling dynamics. By integrating FFP order systems into our newly developed model, we seek a more realistic approach to ecological processes, leveraging past data to enhance predictive accuracy and improve the interpretation of long-term environmental impacts. To the best of our knowledge, no existing mathematical model has yet applied the FFP operator to the study of plastic waste in the ocean, as presented in [1]. The highlight of this study is the investigation of the model, which shows how the considered model may be controlled and stabilized. To achieve this aim, we first find the equilibrium points and analyze the stability of the proposed model. The existence and uniqueness of results are investigated, as well as various Ulam stabilities are used to examine the stability of the solutions. Furthermore, we employ four numerical methods to derive the numerical schemes, including the decomposition technique, the Adams-Bashforth method, the Newton polynomial method, and the predictor-corrector method. The development of control strategies for the proposed model is guided by observations derived from illustrative graphical numerical simulations. Therefore, this research will contribute to dynamic behavior analysis and theoretical conclusions in the following perspectives and structures: Section 1 presents the introduction, background, and literature review. Section 2 shows two subsections of the basic concepts of the FFP operator used in the model and the determination of the proposed model. The model analysis in the context of the positivity and boundedness of the solution and the stability of the equilibrium points (EPs) using the basic reproduction number (BRN) are examined in Section 3. The sensitivity analysis is also analyzed in this section. In Section 4, the existence and uniqueness of the solution are investigated via Banach's

fixed-point theorem. Section 5 proves the UH stability and UHR stability of the proposed model. In Section 6, the numerical scheme is verified to obtain the numerical simulations shown graphically in Section 7. Finally, the significant findings of our investigation are concluded in the last part.

2. Basic materials and preliminaries

2.1. Mathematical materials

Here, we gives some essential definitions of the FFP operators of the proposed model under study. For more details, see [11, 23–26].

Definition 2.1 ([11, 23]). *Suppose that $x(t)$ is a continuous function in (a, b). Then, the FFP integral of $x(t)$ of order α in the RL sense is defined as:*

$$ {}_0^{FFP}\mathcal{I}_t^{\alpha,\beta}x(t) = \frac{\beta}{\Gamma(\alpha)}\int_0^t (t-s)^{\alpha-1}s^{\beta-1}x(s)ds, \quad \alpha,\beta \in (n-1,n], \quad n \in \mathbb{N}. \tag{2.1} $$

If $\beta = 1$, Eq (2.1) can be reduced to

$$ {}_0^{RL}\mathcal{I}_t^{\alpha}x(t) = \frac{1}{\Gamma(\alpha)}\int_0^t (t-s)^{\alpha-1}x(s)ds. \tag{2.2} $$

Definition 2.2 ([11, 23]). *Suppose that $x(t)$ is a continuous function. Then, the fractal (Hausdorff) derivative of $x(t)$ with respect to t^β (fractal dimension) is defined as*

$$ \frac{dx(s)}{ds^\beta} = \lim_{t\to s}\frac{x(t)-x(s)}{t^\beta - s^\beta}. $$

Definition 2.3 ([11, 23]). *Suppose that $x(t)$ is a continuous function which is fractal differentiable in (a, b) via $\alpha \in (n-1, n]$, $n \in \mathbb{N}$. Then, the FFP derivative of $x(t)$ of α and $\beta \in (n-1, n]$ in the RL sense with the power law kernel defined as*

$$ {}_0^{FFP_{RL}}\mathfrak{D}_t^{\alpha,\beta}x(t) = \frac{1}{\Gamma(n-\alpha)}\frac{d}{dt^\beta}\int_0^t (t-s)^{n-\alpha-1}x(s)ds. $$

If $\beta = 1$ and $n = 1$, Eq (2.3) can be reduced to

$$ {}_0^{RL}\mathfrak{D}_t^{\alpha}x(t) = \frac{1}{\Gamma(1-\alpha)}\frac{d}{dt}\int_0^t (t-s)^{-\alpha}x(s)ds = \frac{d}{dt}\left({}_0^{RL}\mathcal{I}_t^{1-\alpha}x(t)\right). \tag{2.3} $$

Definition 2.4 ([11, 23]). *Suppose that $x(t)$ is a continuous function which is fractal differentiable in (a, b) with $\alpha \in (n-1, n]$, $n \in \mathbb{N}$. Then, the FFP derivative of $x(t)$ of α and $\beta \in (n-1, n]$ in the Caputo sense with the power law kernel defined as*

$$ {}_0^{FFP_C}\mathfrak{D}_t^{\alpha,\beta}x(t) = \frac{1}{\Gamma(n-\alpha)}\int_0^t (t-s)^{n-\alpha-1}\frac{dx(s)}{ds^\beta}ds. \tag{2.4} $$

If $\beta = 1$ and $n = 1$, Eq (2.4) can be reduced to

$$ {}_0^{C}\mathfrak{D}_t^{\alpha}x(t) = \frac{1}{\Gamma(1-\alpha)}\int_0^t (t-s)^{-\alpha}x'(s)ds = {}_0^{RL}\mathcal{I}_t^{1-\alpha}\left(\frac{dx(t)}{dt}\right). \tag{2.5} $$

In addition, putting $n = 1$ into (2.4)*, Eq* (2.4) *can be re-written as follows:*

$$ {}_0^{FFP_C}\mathfrak{D}_t^{\alpha,\beta}x(t) = \frac{1}{\beta t^{\beta-1}}\,{}_0^{C}\mathfrak{D}_t^{\alpha}x(t). \tag{2.6}$$

Next, we present the important properties of Definition 2.4, which are used in this paper.

Property 2.5. *Assume that $x, y : [a, b] \to \mathbb{R}$ are such that ${}_0^{FFP_C}\mathfrak{D}_t^{\alpha,\beta}x(t)$ and ${}_0^{FFP_C}\mathfrak{D}_t^{\alpha,\beta}y(t)$ exist almost everywhere and $k_i \in \mathbb{R}$, $i = 1, 2$. Then, ${}_0^{FFP_C}\mathfrak{D}_t^{\alpha,\beta}\left[x(t) \pm y(t)\right]$ exist almost everywhere, and*

$$ {}_0^{FFP_C}\mathfrak{D}_t^{\alpha,\beta}\left[k_1x(t) \pm k_2y(t)\right] = k_1\,{}_0^{FFP_C}\mathfrak{D}_t^{\alpha,\beta}x(t) \pm k_2\,{}_0^{FFP_C}\mathfrak{D}_t^{\alpha,\beta}y(t).$$

Proof. By applying Definition 2.4, we omit the proof. □

The stability study of nonlinear differential systems in the context of the FFP Caputo derivative operator is related to the following definitions.

Definition 2.6. *The constant x^* is an equilibrium of FFP differential system ${}_0^{FFP_C}\mathfrak{D}_t^{\alpha,\beta}x(t) = f(t, x(t))$ if and only if $f(t, x^*) = 0$ for all $t \geq 0$.*

The following lemma extends the Volterra-type Lyapunov function to fractional-order systems [24] and uses an inequality to approximate the $\mathbb{FFP}$ derivatives in the Caputo sense of the function.

Lemma 2.7. *Assume that $x(t) \in \mathbb{R}^+$ is a continuous and differentiable function. For any $t \geq t_0$, then*

$$ {}_0^{FFP_C}\mathfrak{D}_t^{\alpha,\beta}\left[x(t) - x^* - x^*\ln\left(\frac{x(t)}{x^*}\right)\right] \leq \left(1 - \frac{x^*}{x(t)}\right){}_0^{FFP_C}\mathfrak{D}_t^{\alpha,\beta}x(t), \quad x^* \in \mathbb{R}^+, \quad \alpha,\beta \in (0, 1).$$

Proof. Using Property 2.5, yields that

$$ {}_0^{FFP_C}\mathfrak{D}_t^{\alpha,\beta}x(t) - {}_0^{FFP_C}\mathfrak{D}_t^{\alpha,\beta}x^* - x^*\,{}_0^{FFP_C}\mathfrak{D}_t^{\alpha,\beta}\left[\ln\frac{x(t)}{x^*}\right] \leq \left(\frac{x(t) - x^*}{x(t)}\right){}_0^{FFP_C}\mathfrak{D}_t^{\alpha,\beta}x(t).$$

Since ${}_0^{FFP_C}\mathfrak{D}_t^{\alpha,\beta}(C) = 0$, where C is an arbitrary constant, one has

$$ x(t)\,{}_0^{FFP_C}\mathfrak{D}_t^{\alpha,\beta}x(t) - x^*x(t)\,{}_0^{FFP_C}\mathfrak{D}_t^{\alpha,\beta}\left[\ln\frac{x(t)}{x^*}\right] \leq (x(t) - x^*)\,{}_0^{FFP_C}\mathfrak{D}_t^{\alpha,\beta}x(t). \tag{2.7}$$

Using (2.7), implies that

$$ {}_0^{FFP_C}\mathfrak{D}_t^{\alpha,\beta}x(t) - x(t)\,{}_0^{FFP_C}\mathfrak{D}_t^{\alpha,\beta}\left[\ln\frac{x(t)}{x^*}\right] \leq 0. \tag{2.8}$$

From Definition 2.2, we get

$$ \frac{dx(t)}{dt^\beta} = \frac{x'(t)}{\beta t^{\beta-1}} \qquad \text{and} \qquad \frac{d}{dt^\beta}\left[\ln\frac{x(t)}{x^*}\right] = \frac{x'(t)}{\beta t^{\beta-1}x(t)}. \tag{2.9}$$

Using Definition 2.2 with properties (2.9), inequality (2.8) can be obtained as

$$ \frac{1}{\Gamma(1-\alpha)}\int_0^t \frac{dx(s)}{ds^\beta}(t-s)^{-\alpha}ds - \frac{x(t)}{\Gamma(1-\alpha)}\int_0^t \frac{d}{ds^\beta}\left[\ln\frac{x(s)}{x^*}\right](t-s)^{-\alpha}ds$$

$$= \frac{1}{\Gamma(1-\alpha)}\int_0^t \frac{x'(s)}{\beta s^{\beta-1}}(t-s)^{-\alpha}ds - \frac{x(t)}{\Gamma(1-\alpha)}\int_0^t \frac{x'(s)}{\beta s^{\beta-1}x(s)}(t-s)^{-\alpha}ds$$
$$= \frac{1}{\Gamma(1-\alpha)}\int_0^t \left(\frac{x(s)-x(t)}{x(s)}\right)\frac{x'(s)}{\beta s^{\beta-1}(t-s)^{\alpha}}ds \leq 0. \tag{2.10}$$

Setting $x(t)w(s) = x(s) - x(t)$, we have $x(t)w'(s) = x'(s)$. From inequality (2.10), we get

$$\frac{1}{\Gamma(1-\alpha)}\int_0^t x(t)\left(1-\frac{1}{w(s)+1}\right)\frac{w'(s)}{\beta s^{\beta-1}(t-s)^{\alpha}}ds \leq 0.$$

Using the technique of integrating by parts in the last integral, implies that

$$\begin{aligned}
&\frac{1}{\Gamma(1-\alpha)}\int_0^t x(t)\left(1-\frac{1}{w(s)+1}\right)\frac{w'(s)}{\beta s^{\beta-1}(t-s)^{\alpha}}ds\\
=\ &\left[\left(\frac{s^{1-\beta}(t-s)^{-\alpha}}{\Gamma(1-\alpha)}\right)\Big(x(t)\Big(w(s)-\ln(w(s)+1)\Big)\Big)\right]_{s=0}^{s=t}\\
&-\frac{1}{\Gamma(1-\alpha)}\int_0^t \Big(\frac{\alpha s}{t-s}+1-\beta\Big)\frac{x(t)}{s^{\beta}(t-s)^{\alpha}}\Big(w(s)-\ln(w(s)+1)\Big)ds\\
=\ &\left[\left(\frac{s^{1-\beta}(t-s)^{-\alpha}}{\Gamma(1-\alpha)}\right)\Big(x(t)\Big(w(s)-\ln(w(s)+1)\Big)\Big)\right]_{s=t}\\
&-\frac{1}{\Gamma(1-\alpha)}\int_0^t \Big(\frac{\alpha s}{t-s}+1-\beta\Big)\frac{x(t)}{s^{\beta}(t-s)^{\alpha}}\Big(w(s)-\ln(w(s)+1)\Big)ds \leq 0.
\end{aligned} \tag{2.11}$$

It is easy to see that the first term of (2.11) has hesitancy at time $s = t$. Next, we show the synonymous limit:

$$\lim_{s\to t}\left[\left(\frac{s^{1-\beta}(t-s)^{-\alpha}}{\Gamma(1-\alpha)}\right)\Big(x(t)\Big(w(s)-\ln(w(s)+1)\Big)\Big)\right] = \frac{1}{\Gamma(1-\alpha)}\lim_{s\to t}\left[\frac{x(s)-x(t)-x(t)\ln\frac{x(s)}{x(t)}}{s^{\beta-1}(t-s)^{\alpha}}\right].$$

Applying L'Hopital's rule, inequality (2.11) can be reduced to

$$-\frac{1}{\Gamma(1-\alpha)}\int_0^t \Big(\frac{\alpha s}{t-s}+1-\beta\Big)\frac{x(t)\Big(w(s)-\ln(w(s)+1)\Big)}{s^{\beta}(t-s)^{\alpha}}ds \leq 0,$$

or

$$-\int_0^t \Big(\frac{\alpha s}{t-s}+1-\beta\Big)\frac{\Big(x(s)-x(t)-x(t)\ln\frac{x(s)}{x(t)}\Big)}{s^{\beta}(t-s)^{\alpha}\Gamma(1-\alpha)}ds \leq 0. \tag{2.12}$$

It is easy to see that (2.12) holds. The proof is done. □

Remark 2.8. *For the family of the Volterra-type Lyapunov function, that is,*

$$L(x_1, x_2, \ldots, x_n) = \sum_{i=1}^{n} c_i\left(x_i - x_i^* - x_i^*\ln\frac{x_i}{x_i^*}\right),$$

we have the following property:

$${}_0^{FFP_C}\mathfrak{D}_t^{\alpha,\beta}L(x_1, x_2, \ldots, x_n) \leq \sum_{i=1}^{n} c_i\left(1-\frac{x_i^*}{x_i(t)}\right){}_0^{FFP_C}\mathfrak{D}_t^{\alpha,\beta}x_i(t).$$

Proof. The proof is straightforward by applying Property 2.5 and Lemma 2.7. □

Definition 2.9 ([25]). *The Laplace transform of a function $x(t)$, $t \geq 0$, is given as follows:*

$$\mathcal{L}\{x(t)\} = X(s) = \int_0^\infty e^{-st} x(t) dt. \tag{2.13}$$

By applying Definition 2.9, we obtain that

$$\mathcal{L}\left\{t^{\mu-1}\mathbb{E}_{\alpha,\mu}\left(-\delta t^\alpha\right)\right\} = \frac{s^{\alpha-\mu}}{s^\alpha + \delta} \quad \text{where} \quad \mathbb{E}_{\alpha,\mu}(t) = \sum_{k=0}^{\infty} \frac{t^k}{\Gamma(k\alpha + \mu)},$$

and

$$\mathcal{L}\left\{{}_0^C\mathfrak{D}_t^\alpha x(t)\right\} = s^\alpha X(s) - \sum_{j=0}^{n-1} s^{\alpha-j-1} x^{(j)}(0).$$

Definition 2.10 ([26]). *The β-Laplace transform of a function $x : [0, \infty) \to \mathbb{R}$ is provided by*

$$\mathcal{L}_\beta\{x(t)\} = \int_0^\infty \mathbb{E}_\beta(-s, t) x(t) d_\beta t = \int_0^\infty \exp\left(-s\frac{t^\beta}{\beta}\right) x(t) d_\beta t, \quad \beta \in (0, 1]. \tag{2.14}$$

2.2. The fractal-fractional-order extension of the FFP-WPO model

This section refers to the integer order of the WPO model presented in [1], which studied the management of waste plastic on the ocean surface. This model is classified into three compartments: waste plastic material ($W(t)$), marine debris ($M(t)$), and reprocessing or recycling ($R(t)$), which is given as

$$\begin{cases} \dfrac{dW(t)}{dt} = \Lambda - (\gamma + bM(t))\, W(t) + \mu R(t), \\ \dfrac{dM(t)}{dt} = (bW(t) - a)\, M(t), \\ \dfrac{dR(t)}{dt} = aM(t) + \gamma W(t) - (\mu + \theta)\, R(t), \end{cases} \tag{2.15}$$

under the positive conditions $W(0) = W_0 \geq 0$, $M(0) = M_0 \geq 0$, $R(0) = R_0 \geq 0$. The descriptions of unknown parameters are as follows: b denotes the waste rate to become marine, a denotes the marine debris rate to recycle, Λ denotes the new waste rate, which is to be reproduced, θ denotes the recycled waste rate to be lost, μ denotes the recycled waste rate to be reproduced as new waste, and γ denotes the waste rate to be recycled directly without using marine debris. The relation diagram of the population flow among these compartments is shown in Figure 1.

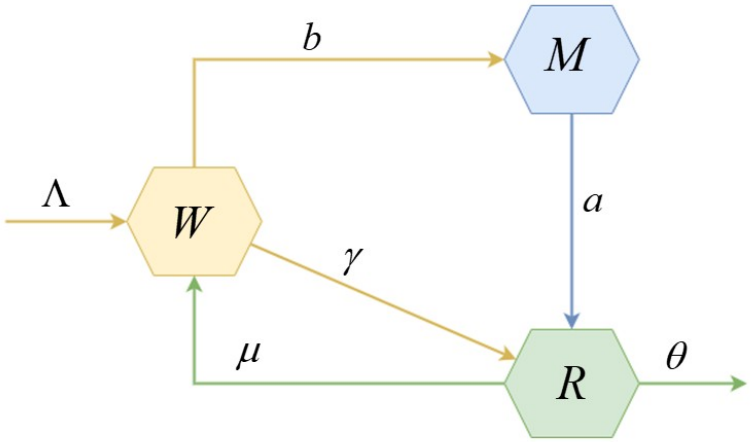

Figure 1. The diagram of the proposed WPO model (2.15).

A summary of probable alterations and transmissions between compartments W, M, and R as provided in Table 1.

Table 1. All potential transmissions and their rates for compartments W, M, and R as shown in Figure 1.

Change/Transmission	Rate
Compartment W	
Reproduction of new waste.	$+\Lambda$
Converting the waste into marine debris.	$-bMW$
Direct recycling of the waste.	$-\gamma W$
Reproduction of the new waste from recycled materials.	$+\mu R$
Compartment M	
Converting the marine debris from the waste.	$+\gamma W$
Recycling the marine debris.	$-aM$
Compartment R	
Recycling the waste.	$+\gamma W$
Recycling the materials from the marine debris.	$+aM$
Changing the recycled materials to the waste.	$-\mu R$
The recycled materials to be lost.	$-\theta R$

Here, we further develop the WPO model (2.15) utilizing the FFP derivative operator with the power law kernal ${}_0^{FFP_C}\mathfrak{D}_t^{\alpha,\beta}$ as follows:

$$\begin{cases} {}_0^{FFP_C}\mathfrak{D}_t^{\alpha,\beta} W(t) = \Lambda - (\gamma + bM(t))\, W(t) + \mu R(t), \\ {}_0^{FFP_C}\mathfrak{D}_t^{\alpha,\beta} M(t) = (bW(t) - a)\, M(t), \\ {}_0^{FFP_C}\mathfrak{D}_t^{\alpha,\beta} R(t) = aM(t) + \gamma W(t) - (\mu + \theta)\, R(t), \end{cases} \tag{2.16}$$

with the conditions $W(0) = W_0 \geq 0$, $M(0) = M_0 \geq 0$, $R(0) = R_0 \geq 0$. The model (2.16) is called the FFP-WPO model.

3. Foundation analysis

This part discusses the positivity, boundedness, and equilibria analysis of the FFP-WPO model (2.16).

3.1. Positivity and boundedness

To prove the positivity of the considered model, we set

$$\mathbb{R}^3_+ = \{\mathcal{G} \in \mathbb{R}^3 : \mathcal{G} \geq 0 \quad \text{and} \quad \mathcal{G}(t) = (W(t), R(t), M(t))^{\mathcal{T}}\}. \tag{3.1}$$

Theorem 3.1. *A solution $\mathcal{G}$ of the FFP-WPO model* (2.16) *exists and bounded in $\mathbb{R}^3_+$. Furthermore, the solution will be non-negative.*

Proof. Obviously, for the time interval $(0, \infty)$, the solution for the FFP-WPO model (2.16) exists. From this model, we have

$$\begin{cases} {}^{FFP_C}_{0}\mathfrak{D}^{\alpha,\beta}_t W(t) = \Lambda + \mu R(t) \geq 0, \\ {}^{FFP_C}_{0}\mathfrak{D}^{\alpha,\beta}_t M(t) = bM(t)W(t) \geq 0, \\ {}^{FFP_C}_{0}\mathfrak{D}^{\alpha,\beta}_t R(t) = aM(t) + \gamma W(t) \geq 0. \end{cases} \tag{3.2}$$

Since all of the parameters and initial conditions of the proposed model are positive in $\mathbb{R}^3_+$, then, for all $t \geq 0$, the solutions are all non-negative. That is to say, if we start with initial data in $\mathbb{R}^3_+$, the solutions will remain in $\mathbb{R}^3_+$. Now, we provide $V(t) = 2W(t) + 2M(t) + R(t)$. From the FFP-WPO model (2.16), we obtain

$${}^{FFP_C}_{0}\mathfrak{D}^{\alpha,\beta}_t V(t) = 2\Lambda - \gamma W - aM - (\theta - \mu)R \leq 2\Lambda - \rho V(t), \tag{3.3}$$

where $0 < \rho \leq \min\{\frac{\gamma}{2}, \frac{a}{2}, \theta - \mu\}$. By using relation (2.6), Eq (3.3) can rewritten in the following form:

$${}^{C}_{0}\mathfrak{D}^{\alpha}_t V(t) \leq \beta t^{\beta-1}(2\Lambda - \rho V(t)). \tag{3.4}$$

Applying Definition 2.9 in (3.4) yields that

$$V(t) = \mathbb{E}_{\alpha,1}(-\rho t^{\alpha})V(0) + 2\Lambda\Gamma(\beta + 1)t^{\beta+\alpha-1}\mathbb{E}_{\alpha,\beta+\alpha}(-\rho t^{\alpha}). \tag{3.5}$$

Thus, $\lim_{t\to\infty} V(t) \leq 2\Lambda/\rho$. Hence, the feasible region for the FFP-WPO model (2.16) is given as

$$\Omega = \left\{\mathcal{G} := (W, M, R) \in \mathbb{R}^3, \mathcal{G} \geq 0 \quad \text{and} \quad V(t) \leq \frac{2\Lambda}{\rho}\right\},$$

and this proves the boundedness of the solution of the FFP-WPO model (2.16). □

3.2. Equilibria and stability of the FFP-WPO model (2.16)

In this subsection, we investigate EPs of the FFP-WPO model (2.16) and analyze their stability. By setting the right side of three equations is zero, the system has two possible EPs. They are:

- The boundary equilibrium point (BEP) or marine debris-free equilibrium: $\mathfrak{E}^*_0 = \left(\frac{\Lambda(\mu+\theta)}{\theta\gamma}, 0, \frac{\Lambda}{\theta}\right)$ exist for all parametric values.

- The interior equilibrium point (IEP) or marine debris-included equilibrium: $\mathfrak{E}_1^* = \left(\frac{a}{b}, \frac{(\mu+\theta)b\Lambda - a\gamma\theta}{\theta ba}, \frac{\Lambda}{\theta}\right)$ exist if $P_0 := \frac{b\Lambda(\mu+\theta)}{a\gamma\theta} > 1$ where P_0 is BRN, which is computed by the dominating eigenvalue of the next-generation matrix [27].

Theorem 3.2. *If $P_0 < 1$, then the marine debris-free equilibrium $\mathfrak{E}_0^*$ is locally asymptotically stable (LAS) with necessary and sufficient conditions*

$$|arg(\lambda_i)| > \frac{\eta\pi}{2}, \quad i = 1, 2, 3, \tag{3.6}$$

otherwise it is unstable.

Proof. The Jacobian matrix $\mathbb{J}$ at $\mathfrak{E}_0^*$ is defined by

$$\mathbb{J}(\mathfrak{E}_0^*) = \begin{pmatrix} -\gamma & -\frac{b\Lambda(\mu+\theta)}{\theta\gamma} & \mu \\ 0 & \frac{b\Lambda(\mu+\theta)}{\theta\gamma} - a & 0 \\ \gamma & a & -\mu-\theta \end{pmatrix}. \tag{3.7}$$

Then, the eigenvalues associated with the Jacobian matrix computed around $\mathfrak{E}_0^*$ are

$$\lambda_1 = \frac{b\Lambda(\mu+\theta)}{\theta\gamma} - a, \quad \lambda_{2,3} = \frac{1}{2}\left(-(\mu+\theta+\gamma) \pm \sqrt{(\mu+\theta+\gamma)^2 - 4(\gamma(\mu+\theta)+\mu\gamma)}\right).$$

From our assumption $P_0 < 1$, implies that $\lambda_1 < 0$. It is also easy to see that $\lambda_2 < 0$ and $\lambda_3 < 0$. Since all eigenvalues have negative real parts, this assures condition (3.6) is satisfied for any $\eta \in (0, 1]$. Hence, $\mathfrak{E}_0^*$ is LAS. □

Theorem 3.3. *If $P_0 > 1$, then the marine debris-included equilibrium $\mathfrak{E}_1^*$ is LAS, otherwise it is unstable.*

Proof. The Jacobian matrix $\mathbb{J}$ at $\mathfrak{E}_1^*$ is defined by

$$\mathbb{J}(\mathfrak{E}_1^*) = \begin{pmatrix} -\gamma - C & -a & \mu \\ C & 0 & 0 \\ \gamma & a & -\mu-\theta \end{pmatrix}, \quad \text{where} \quad C = \frac{b\Lambda(\mu+\theta) - a\gamma\theta}{\theta a} > 0. \tag{3.8}$$

Note that if $P_0 > 1$, then $C > 0$. The characteristic equation at $\mathfrak{E}_1^*$ is obtained as follows:

$$\lambda^3 + a_2\lambda^2 + a_1\lambda + a_0 = 0, \tag{3.9}$$

where $a_2 = \mu+\theta+\gamma+C$, $a_1 = (\gamma+C)(\mu+\theta) - \gamma\mu + aC$, and $a_0 = aC\theta$. It is easy to see that $a_i > 0$, $i = 1$, 2, 3, and $a_1a_2 > a_0$. By the Routh-Hurwitz criteria [28], we can conclude that all real eigenvalues and all real parts of the complex conjugate eigenvalues of (3.9) are negative. Therefore, $\mathfrak{E}_1^*$ is LAS. □

Theorem 3.4. *The marine debris-free equilibrium $\mathfrak{E}_0^*$ is globally asymptotically stable (GAS) if $P_0 \leq 1$, otherwise it is unstable.*

Proof. Let us consider the positive definite Lyapunov function $\mathfrak{L}_0(t)$ provided by

$$\mathfrak{L}_0(t) = \frac{W_0^*}{\gamma}\psi\left(\frac{W(t)}{W_0^*}\right) + \frac{M_0^*}{a}\psi\left(\frac{M(t)}{M_0^*}\right) + \frac{R_0^*}{\mu+\theta}\psi\left(\frac{R(t)}{R_0^*}\right), \tag{3.10}$$

where $\psi(u) = u - \ln(u) - 1$, for all $u > 0$. Acting the operator ${}_0^{\mathbb{FFP}_C}\mathfrak{D}_t^{\alpha,\beta}$ on (3.10), we have

$$\begin{aligned}
{}_0^{FFP_C}\mathfrak{D}_t^{\alpha,\beta}\mathfrak{L}_0(t) &= \frac{W_0^*}{\gamma}{}_0^{FFP_C}\mathfrak{D}_t^{\alpha,\beta}\left[\psi\left(\frac{W(t)}{W_0^*}\right)\right] + \frac{M_0^*}{a}{}_0^{FFP_C}\mathfrak{D}_t^{\alpha,\beta}\left[\psi\left(\frac{M(t)}{M_0^*}\right)\right] + \frac{R_0^*}{\mu+\theta}{}_0^{FFP_C}\mathfrak{D}_t^{\alpha,\beta}\left[\psi\left(\frac{R(t)}{R_0^*}\right)\right] \\
&= \frac{1}{\gamma}{}_0^{FFP_C}\mathfrak{D}_t^{\alpha,\beta}\left[W(t) - W_0^*\ln\left(\frac{W(t)}{W_0^*}\right) - W_0^*\right] + \frac{1}{a}{}_0^{FFP_C}\mathfrak{D}_t^{\alpha,\beta}\left[M(t) - M_0^*\ln\left(\frac{M(t)}{M_0^*}\right) - M_0^*\right] \\
&\quad + \frac{1}{\mu+\theta}{}_0^{FFP_C}\mathfrak{D}_t^{\alpha,\beta}\left[R(t) - R_0^*\ln\left(\frac{R(t)}{R_0^*}\right) - R_0^*\right].
\end{aligned}$$

Using Lemma 2.7, we get

$$\begin{aligned}
&{}_0^{FFP_C}\mathfrak{D}_t^{\alpha,\beta}\mathfrak{L}_0(t) \\
&\leq \frac{1}{\gamma}\left(1 - \frac{W_0^*}{W(t)}\right){}_0^{FFP_C}\mathfrak{D}_t^{\alpha,\beta}W(t) + \frac{1}{a}\left(1 - \frac{M_0^*}{M(t)}\right){}_0^{FFP_C}\mathfrak{D}_t^{\alpha,\beta}M(t) + \frac{1}{\mu+\theta}\left(1 - \frac{R_0^*}{R(t)}\right){}_0^{FFP_C}\mathfrak{D}_t^{\alpha,\beta}R(t) \\
&\leq \frac{1}{\gamma}\left(1 - \frac{W_0^*}{W(t)}\right)\left[\Lambda - (\gamma + bM(t))\,W(t) + \mu R(t)\right] + \frac{1}{a}\left(1 - \frac{M_0^*}{M(t)}\right)\left[(bW(t) - a)\,M(t)\right] \\
&\quad + \frac{1}{\mu+\theta}\left(1 - \frac{R_0^*}{R(t)}\right)\left[aM(t) + \gamma W(t) - (\mu+\theta)\,R(t)\right].
\end{aligned} \tag{3.11}$$

Since $\mathfrak{E}_0^* = (W_0^*, M_0^*, R_0^*)$, we can write the following relationship between each point:

$$\Lambda - bM_0^*W_0^* + \mu R_0^* = \gamma W_0^*, \quad bW_0^*M_0^* = aM_0^*, \quad aM_0^* + \gamma W_0^* = (\mu+\theta)\,R_0^*. \tag{3.12}$$

Substituting (3.12) into (3.11), implies that

$${}_0^{FFP_C}\mathfrak{D}_t^{\alpha,\beta}\mathfrak{L}_0(t) \leq -\left\{\frac{(W(t) - W_0^*)^2}{W(t)} + \frac{(M(t) - M_0^*)^2}{M(t)} + \frac{(R(t) - R_0^*)^2}{R(t)}\right\}.$$

Then, ${}_0^{FFP_C}\mathfrak{D}_t^{\alpha,\beta}\mathfrak{L}_0(t) \leq 0$. Clearly, ${}_0^{FFP_C}\mathfrak{D}_t^{\alpha,\beta}\mathfrak{L}_0(t) = 0$ if and only if $W(t) = W_0^*$, $M(t) = M_0^*$, and $R(t) = R_0^*$. Hence, the largest invariant set contained in $\{(W, M, R)|_0^{\mathbb{FFP}_C}\mathfrak{D}_t^{\alpha,\beta}\mathfrak{L}_0(t) = 0\}$ is the singleton $\{\mathfrak{E}_0^*\}$. By LaSalle's invariance principle [29], we deduce that $\mathfrak{E}_0^*$ is GAS for $P_0 \leq 1$. □

Theorem 3.5. *The marine debris-included equilibrium $\mathfrak{E}_1^*$ is GAS if $P_0 > 1$, otherwise it is unstable.*

Proof. Let us consider the positive definite Lyapunov function $\mathfrak{L}_1(t)$ provided by

$$\mathfrak{L}_1(t) = \frac{W_1^*}{\gamma}\psi\left(\frac{W(t)}{W_1^*}\right) + \frac{M_1^*}{a}\psi\left(\frac{M(t)}{M_1^*}\right) + \frac{R_1^*}{\mu+\theta}\psi\left(\frac{R(t)}{R_1^*}\right), \tag{3.13}$$

where $\psi(u) = u - \ln(u) - 1$, for all $u > 0$. Acting the operator ${}_0^{\mathbb{FFP}_C}\mathfrak{D}_t^{\alpha,\beta}$ on (3.13), we have

$$\begin{aligned}
{}_0^{FFP_C}\mathfrak{D}_t^{\alpha,\beta}\mathfrak{L}_1(t) &= \frac{W_1^*}{\gamma}{}_0^{FFP_C}\mathfrak{D}_t^{\alpha,\beta}\left[\psi\left(\frac{W(t)}{W_1^*}\right)\right] + \frac{M_1^*}{a}{}_0^{FFP_C}\mathfrak{D}_t^{\alpha,\beta}\left[\psi\left(\frac{M(t)}{M_1^*}\right)\right] + \frac{R_1^*}{\mu+\theta}{}_0^{FFP_C}\mathfrak{D}_t^{\alpha,\beta}\left[\psi\left(\frac{R(t)}{R_1^*}\right)\right]
\end{aligned}$$

$$= \frac{1}{\gamma}{}_0^{FFP_C}\mathfrak{D}_t^{\alpha,\beta}\left[W(t) - W_1^* \ln\left(\frac{W(t)}{W_1^*}\right) - W_1^*\right] + \frac{1}{a}{}_0^{FFP_C}\mathfrak{D}_t^{\alpha,\beta}\left[M(t) - M_1^* \ln\left(\frac{M(t)}{M_1^*}\right) - M_1^*\right]$$
$$+ \frac{1}{\mu+\theta}{}_0^{FFP_C}\mathfrak{D}_t^{\alpha,\beta}\left[R(t) - R_1^* \ln\left(\frac{R(t)}{R_1^*}\right) - R_1^*\right].$$

Using Lemma 2.7, we get

$$\begin{aligned}
&{}_0^{FFP_C}\mathfrak{D}_t^{\alpha,\beta}\mathfrak{L}_1(t)\\
\leq\ & \frac{1}{\gamma}\left(1 - \frac{W_1^*}{W(t)}\right){}_0^{FFP_C}\mathfrak{D}_t^{\alpha,\beta}W(t) + \frac{1}{a}\left(1 - \frac{M_1^*}{M(t)}\right){}_0^{FFP_C}\mathfrak{D}_t^{\alpha,\beta}M(t) + \frac{1}{\mu+\theta}\left(1 - \frac{R_1^*}{R(t)}\right){}_0^{FFP_C}\mathfrak{D}_t^{\alpha,\beta}R(t)\\
\leq\ & \frac{1}{\gamma}\left(1 - \frac{W_1^*}{W(t)}\right)\left[\Lambda - (\gamma + bM(t))\,W(t) + \mu R(t)\right] + \frac{1}{a}\left(1 - \frac{M_1^*}{M(t)}\right)\left[(bW(t) - a)\,M(t)\right]\\
&+ \frac{1}{\mu+\theta}\left(1 - \frac{R_1^*}{R(t)}\right)\left[aM(t) + \gamma W(t) - (\mu+\theta)\,R(t)\right]. \qquad (3.14)
\end{aligned}$$

Since $\mathfrak{E}_1^* = (W_1^*, M_1^*, R_1^*)$, we can write the following relationship between each point:

$$\Lambda - bM_1^*W_1^* + \mu R_1^* = \gamma W_1^*, \quad bW_1^*M_1^* = aM_1^*, \quad aM_1^* + \gamma W_1^* = (\mu+\theta)\,R_1^*. \qquad (3.15)$$

Inserting (3.15) into (3.14), implies that

$${}_0^{FFP_C}\mathfrak{D}_t^{\alpha,\beta}\mathfrak{L}_1(t) \leq -\left\{\frac{(W(t) - W_1^*)^2}{W(t)} + \frac{(M(t) - M_1^*)^2}{M(t)} + \frac{(R(t) - R_1^*)^2}{R(t)}\right\}.$$

Then, ${}_0^{FFP_C}\mathfrak{D}_t^{\alpha,\beta}\mathfrak{L}_1(t) \leq 0$. Clearly, ${}_0^{FFP_C}\mathfrak{D}_t^{\alpha,\beta}\mathfrak{L}_1(t) = 0$ if and only if $W(t) = W_1^*$, $M(t) = M_1^*$, and $R(t) = R_1^*$. Hence, the largest invariant set contained in $\{(W, M, R)|_0^{FFP_C}\mathfrak{D}_t^{\alpha,\beta}\mathfrak{L}_1(t) = 0\}$ is the singleton $\{\mathfrak{E}_1^*\}$. By LaSalle's invariance principle [29], we deduce that $\mathfrak{E}_1^*$ is GAS for $P_0 > 1$. □

3.3. Sensitivity analysis

Understanding the relevance of the distinct factors related to transmission will aid in decision on the optimal control strategies. Primarily, waste plastic transmission is involved in the basic reproduction number (P_0) and sensitivity forecasts, and thus these parameters have a significant influence on P_0. Sensitivity analysis is used to study the effect of the parameters on the FFP-WPO model (2.16). This approach measures each variable's sensitivity using a metric known as the normalized sensitivity index. It is critical to establish which parameters are the most sensitive, as little changes can have a significant influence on model dynamics. We compute the sensitivity indices of P_0 for its variables (Λ, γ, b, μ, a, and θ) as the value P_0 has a significant influence on the model's behavior. To calculate the normalized sensitivity index ($\Gamma_\omega^{P_0}$), follow these steps [30]:

$$\Gamma_\omega^{P_0} = \frac{\partial P_0}{\partial \omega} \times \frac{\omega}{P_0},$$

where $\omega \in \{\Lambda, \gamma, b, \mu, a, \theta\}$ and $P_0 := (b\Lambda(\mu+\theta))/(a\gamma\theta)$. If the sign of $\Gamma_\omega^{P_0}$ is positive ($\Gamma_\omega^{P_0} > 0$), then the parameter ω has a positive impact on P_0. This yields that the value of P_0 increases if the value of ω increases. On the other hand, if the sign of $\Gamma_\omega^{P_0}$ is negative ($\Gamma_\omega^{P_0} < 0$), then the parameter ω has a

negative impact on P_0 (reverse impact). This implies that the value of P_0 decreases if the value of ω increases. In addition, the magnitude of $\Gamma_{\omega}^{P_0}$ represents the fraction of changes in P_0 due to ω. So, the elasticity index for establishing the sensitivity of P_0 of each parameter is computed as

$$\Gamma_{\Lambda}^{P_0} = \frac{\partial P_0}{\partial \Lambda} \times \frac{\Lambda}{P_0} = \frac{b(\mu+\theta)}{a\gamma\theta} \times \frac{\Lambda}{P_0} = 1, \qquad \Gamma_{\gamma}^{P_0} = \frac{\partial P_0}{\partial \gamma} \times \frac{\gamma}{P_0} = -\frac{b\Lambda(\mu+\theta)}{a\gamma^2\theta} \times \frac{\gamma}{P_0} = -1,$$

$$\Gamma_{b}^{P_0} = \frac{\partial P_0}{\partial b} \times \frac{b}{P_0} = \frac{\Lambda(\mu+\theta)}{a\gamma\theta} \times \frac{b}{P_0} = 1, \qquad \Gamma_{\mu}^{P_0} = \frac{\partial P_0}{\partial \mu} \times \frac{\mu}{P_0} = \frac{b\Lambda}{a\gamma\theta} \times \frac{\mu}{P_0} = \frac{\mu}{\mu+\theta} < 1,$$

$$\Gamma_{a}^{P_0} = \frac{\partial P_0}{\partial a} \times \frac{a}{P_0} = -\frac{b\Lambda(\mu+\theta)}{a^2\gamma\theta} \times \frac{a}{P_0} = -1, \qquad \Gamma_{\theta}^{P_0} = \frac{\partial P_0}{\partial \theta} \times \frac{\theta}{P_0} = -\frac{b\Lambda\mu}{a\gamma\theta^2} \times \frac{\theta}{P_0} = -\frac{\mu}{\mu+\theta} > -1.$$

According to the aforementioned data, increasing the parameters Λ, b, and μ will proportionally have the greatest impact on the number of marine debris $M(t)$ in the ocean. On the other hand, increasing the parameters γ, a, and θ will have the reverse impact on the number of marine debris $M(t)$ in the ocean. The parameter θ represents the pace at which recycled materials $R(t)$ are taken from the ocean's plastic waste management system. Less recycled material means less material returned to plastic waste management, which minimizes the reproduction of marine trash. According to the normalized sensitivity index, the parameter θ has an inverse connection with P_0, and increasing its rate reduces the amount of marine debris. Figure 2 shows a comparison of these parameters using the values $\Lambda = 0.35$, $b = 0.2$, $\mu = 0.3$, $\theta = 0.3$, $a = 0.6$, and $\gamma = 0.4$.

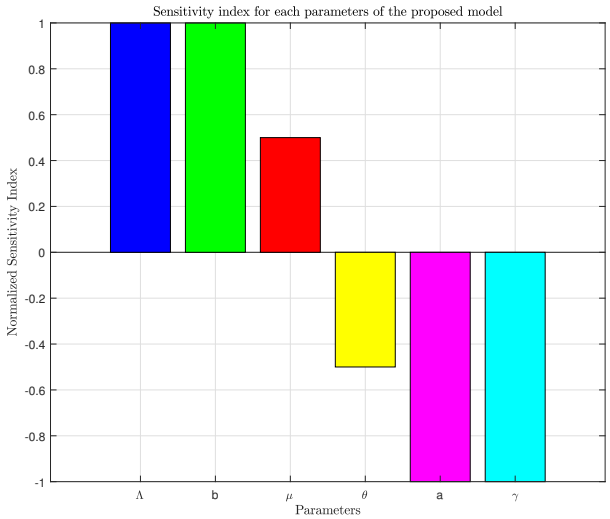

Figure 2. Sensitivity indices for parameters of the FFP-WPO model (2.16).

4. Qualitative results

4.1. Existence and uniqueness result

An analysis of the FFP-WPO model (2.16) will be performed by applying Banach's contraction mapping principle [31]. First, the Banach space on $[0, T]$ for all continuous real-valued functions is given by $\mathbb{X} = C([0, T] \times \mathbb{R}^3, \mathbb{R})$ under the norm $\|\mathbb{U}\| = \|(W, M, R)\| = \|W\| + \|M\| + \|R\|$, where W, M,

$R \in \mathbb{X}$ and $\|W\| = \sup_{t\in[0,T]} |W(t)| = \mathcal{W}^*$, $\|M\| = \sup_{t\in[0,T]} |M(t)| = \mathcal{M}^*$, and $\|R\| = \sup_{t\in[0,T]} |R(t)| = \mathcal{R}^*$. Next, assume $\mathcal{G} \in \mathbb{X}$ and $\mathbb{U} \in C([0,T],\mathbb{R})$. The FFP-WPO model (2.16) can be presented as

$$\begin{cases} {}^{FFP_C}_{0}\mathfrak{D}_t^{\alpha,\beta}\mathbb{U}(t) = \mathcal{G}(t,\mathbb{U}(t)), \quad t \in [0,T], \quad \alpha \in (0,1], \\ \mathbb{U}(0) = \mathbb{U}_0, \end{cases} \tag{4.1}$$

where

$$\mathbb{U} = \begin{pmatrix} W(t) \\ M(t) \\ R(t) \end{pmatrix}, \quad \mathbb{U}(0) = \begin{pmatrix} W(0) \\ M(0) \\ R(0) \end{pmatrix} = \begin{pmatrix} W_0 \\ M_0 \\ R_0 \end{pmatrix}, \quad \mathcal{G}(t,\mathbb{U}(t)) = \begin{pmatrix} \mathcal{G}_1(t,W) \\ \mathcal{G}_2(t,M) \\ \mathcal{G}_3(t,R) \end{pmatrix} = \begin{pmatrix} \Lambda - (\gamma + bM)\, W + \mu R \\ (bW - a)\, M \\ aM - \mu R + \gamma W - \theta R \end{pmatrix}. \tag{4.2}$$

Applying Definitions 2.9 and 2.10 to (4.1), implies that

$$\begin{aligned} \mathcal{L}\left\{{}^{FFP_C}_{0}\mathfrak{D}_t^{\alpha,\beta}\mathbb{U}(t)\right\} &= \mathcal{L}\left\{\mathcal{G}(t,\mathbb{U}(t))\right\}, \\ \frac{1}{\beta}\left(s\mathcal{L}_\beta\left\{\mathbb{U}(t)\right\} - \mathbb{U}(0)\right) &= \mathcal{L}_\beta\left\{\mathcal{L}^{-1}\left\{s^{1-\alpha}\mathcal{L}\left\{\mathcal{G}(t,\mathbb{U}(t))\right\}\right\}\right\}, \\ \mathbb{U}(t) &= \mathbb{U}(0) + \mathcal{L}_\beta^{-1}\left\{\frac{\beta}{s}\mathcal{L}_\beta\left\{\mathcal{L}^{-1}\left\{s^{1-\alpha}\mathcal{L}\left\{\mathcal{G}(t,\mathbb{U}(t))\right\}\right\}\right\}\right\}. \end{aligned} \tag{4.3}$$

From Problem (4.1), Eq (4.3) can be represented in the integral form

$$W(t) = W_0 + \mathcal{L}_\beta^{-1}\left\{\frac{\beta}{s}\mathcal{L}_\beta\left\{\mathcal{L}^{-1}\left\{s^{1-\alpha}\mathcal{L}\left\{\mathcal{G}_1(t,W(t))\right\}\right\}\right\}\right\}, \tag{4.4}$$

$$M(t) = M_0 + \mathcal{L}_\beta^{-1}\left\{\frac{\beta}{s}\mathcal{L}_\beta\left\{\mathcal{L}^{-1}\left\{s^{1-\alpha}\mathcal{L}\left\{\mathcal{G}_2(t,M(t))\right\}\right\}\right\}\right\}, \tag{4.5}$$

$$R(t) = R_0 + \mathcal{L}_\beta^{-1}\left\{\frac{\beta}{s}\mathcal{L}_\beta\left\{\mathcal{L}^{-1}\left\{s^{1-\alpha}\mathcal{L}\left\{\mathcal{G}_3(t,R(t))\right\}\right\}\right\}\right\}. \tag{4.6}$$

Next, we provide an operator $\mathcal{Q} : \mathbb{X} \to \mathbb{X}$ where $\mathcal{Q} = (\mathcal{Q}_1, \mathcal{Q}_2, \mathcal{Q}_3)$. In consideration of (4.4)–(4.6), it follows that

$$\begin{aligned} (\mathcal{Q}_1 W)(t) &= W_0 + \mathcal{L}_\beta^{-1}\left\{\frac{\beta}{s}\mathcal{L}_\beta\left\{\mathcal{L}^{-1}\left\{s^{1-\alpha}\mathcal{L}\left\{\mathcal{G}_1(t,W(t))\right\}\right\}\right\}\right\}, \\ (\mathcal{Q}_2 M)(t) &= M_0 + \mathcal{L}_\beta^{-1}\left\{\frac{\beta}{s}\mathcal{L}_\beta\left\{\mathcal{L}^{-1}\left\{s^{1-\alpha}\mathcal{L}\left\{\mathcal{G}_2(t,M(t))\right\}\right\}\right\}\right\}, \\ (\mathcal{Q}_3 R)(t) &= R_0 + \mathcal{L}_\beta^{-1}\left\{\frac{\beta}{s}\mathcal{L}_\beta\left\{\mathcal{L}^{-1}\left\{s^{1-\alpha}\mathcal{L}\left\{\mathcal{G}_3(t,R(t))\right\}\right\}\right\}\right\}. \end{aligned}$$

Next, we convert the FFP-WPO model (2.16) to the fixed-point problem, that is, $\mathbb{U} = \mathcal{Q}\mathbb{U}$, which will be applied later with a fixed point theory to prove that the FFP-WPO model (2.16) has a solution.

Theorem 4.1. *Assume $\mathcal{G} \in \mathbb{X}$, corresponding with the assumption $(\mathcal{H}_1)$ as follows:*

$(\mathcal{H}_1)$ *There is a constant $L_{\mathcal{G}}^{\max} = \max\{L_{\mathcal{G}_1}, L_{\mathcal{G}_2}, L_{\mathcal{G}_3}\} > 0$ such that*

$$\begin{aligned} &|\mathcal{G}_i(t,W_1(t),M_1(t),R_1(t)) - \mathcal{G}_i(t,W_2(t),M_2(t),R_2(t))| \\ &\leq L_{\mathcal{G}_i}\left(|W_1(t) - W_2(t)| + |M_1(t) - M_2(t)| + |R_1(t) - R_2(t)|\right), \end{aligned} \tag{4.7}$$

where $i = 1, 2, 3$, $W_j, M_j, R_j \in \mathbb{X}$, $j = 1, 2$, and $t \in [0,T]$.

If

$$\beta T^{\alpha+\beta-1} L_{\mathcal{G}}^{\max} < (\alpha+\beta-1)\Gamma(\alpha), \tag{4.8}$$

then the FFP-WPO model (2.16) *has a unique solution.*

Proof. Define a bounded, closed, and convex subset $D_r := \{(W, M, R) \in \mathbb{X} : \|(W, M, R)\|_{\mathbb{X}} \leq r\}$ with a radius r given as

$$r \geq \left(\mathcal{K}_0^{\max} + \frac{\beta T^{\alpha+\beta-1}\mathcal{G}_*^{\max}}{(\alpha+\beta-1)\Gamma(\alpha)}\right)\left(1 - \frac{\beta T^{\alpha+\beta-1} L_{\mathcal{G}}^{\max}}{(\alpha+\beta-1)\Gamma(\alpha)}\right)^{-1},$$

where $\mathcal{K}_0^{\max} = \max\{|W_0|, |M_0|, |R_0|\}$ and $\mathcal{G}_*^{\max} = \max\{\mathcal{G}_1^*, \mathcal{G}_2^*, \mathcal{G}_3^*\}$. Let $\sup_{t\in[0,T]} |\mathcal{G}_i(s,0)| = \mathcal{G}_i^* < +\infty$, $i = 1, 2, 3$. The process is separated into two parts.

Step I. We prove that $\mathcal{Q}D_r \subset D_r$.

For any $W, M, R \in D_r$ and $t \in [0, T]$, we have

$$\begin{aligned}
|(\mathcal{Q}_1 W)(t)| &\leq |W_0| + \beta\mathcal{L}_\beta^{-1}\left\{\frac{1}{s}\mathcal{L}_\beta\left\{\mathcal{L}^{-1}\left\{s^{1-\alpha}\mathcal{L}\{|\mathcal{G}_1(t, W(t))|\}\right\}\right\}\right\} \\
&\leq |W_0| + \beta\mathcal{L}_\beta^{-1}\left\{\frac{1}{s}\mathcal{L}_\beta\left\{\mathcal{L}^{-1}\left\{s^{1-\alpha}\mathcal{L}\{|\mathcal{G}_1(t, W(t)) - \mathcal{G}_1(t,0)| + |\mathcal{G}_1(t,0)|\}\right\}\right\}\right\} \\
&\leq |W_0| + \beta\mathcal{L}_\beta^{-1}\left\{\frac{1}{s}\mathcal{L}_\beta\left\{\mathcal{L}^{-1}\left\{s^{1-\alpha}\mathcal{L}\{1\}\right\}\right\}\right\}(L_{\mathcal{G}_1} r + \mathcal{G}_1^*) \\
&\leq |W_0| + \beta\mathcal{L}_\beta^{-1}\left\{\frac{1}{s}\mathcal{L}_\beta\left\{\mathcal{L}^{-1}\{s^{-\alpha}\}\right\}\right\}(L_{\mathcal{G}_1} r + \mathcal{G}_1^*) \\
&\leq |W_0| + \beta\mathcal{L}_\beta^{-1}\left\{\frac{1}{s}\mathcal{L}_\beta\left\{\frac{t^{\alpha-1}}{\Gamma(\alpha)}\right\}\right\}(L_{\mathcal{G}_1} r + \mathcal{G}_1^*) \\
&\leq |W_0| + \frac{\beta}{\Gamma(\alpha)}\beta^{\frac{\alpha-1}{\beta}}\Gamma\left(\frac{\beta+\alpha-1}{\beta}\right)\mathcal{L}_\beta^{-1}\left\{\frac{1}{s^{2+\frac{\alpha-1}{\beta}}}\right\}(L_{\mathcal{G}_1} r + \mathcal{G}_1^*) \\
&\leq |W_0| + \frac{\beta}{\Gamma(\alpha)}\beta^{\frac{\alpha-1}{\beta}}\Gamma\left(\frac{\beta+\alpha-1}{\beta}\right)\frac{t^{\alpha+\beta-1}}{\beta^{\frac{\alpha+\beta-1}{\beta}}\Gamma\left(1+\frac{\alpha+\beta-1}{\beta}\right)}(L_{\mathcal{G}_1} r + \mathcal{G}_1^*) \\
&\leq |W_0| + \frac{\beta T^{\alpha+\beta-1}\left(L_{\mathcal{G}_1} r + \mathcal{G}_1^*\right)}{(\alpha+\beta-1)\Gamma(\alpha)}.
\end{aligned}$$

This yields that,

$$\|\mathcal{Q}_1 W\|_{\mathbb{X}} \leq |W_0| + \frac{\beta T^{\alpha+\beta-1}\left(L_{\mathcal{G}_1} r + \mathcal{G}_1^*\right)}{(\alpha+\beta-1)\Gamma(\alpha)}.$$

In the same procedure, we also have

$$\|\mathcal{Q}_2 M\|_{\mathbb{X}} \leq |M_0| + \frac{\beta T^{\alpha+\beta-1}\left(L_{\mathcal{G}_2} r + \mathcal{G}_2^*\right)}{(\alpha+\beta-1)\Gamma(\alpha)} \quad \text{and} \quad \|\mathcal{Q}_3 R\|_{\mathbb{X}} \leq |R_0| + \frac{\beta T^{\alpha+\beta-1}\left(L_{\mathcal{G}_3} r + \mathcal{G}_3^*\right)}{(\alpha+\beta-1)\Gamma(\alpha)}.$$

Then,

$$\|(\mathcal{Q}\mathbb{U})(t)\| \leq \mathcal{K}_0^{\max} + \frac{\beta T^{\alpha+\beta-1}\left(L_{\mathcal{G}}^{\max} r + \mathcal{G}_*^{\max}\right)}{(\alpha+\beta-1)\Gamma(\alpha)}.$$

Hence, $QD_r \subset D_r$.

Step II. We show that Q is a contraction.

Let $W_j, M_j, R_j \in D_r$, $j = 1, 2$, for $t \in [0, T]$. This yields that

$$\begin{aligned} |(Q_1W_1)(t) - (Q_1W_2)(t)| &\leq \beta\mathcal{L}_\beta^{-1}\left\{\frac{1}{s}\mathcal{L}_\beta\left\{\mathcal{L}^{-1}\left\{s^{1-\alpha}\mathcal{L}\left\{|\mathcal{G}_1(t, W_1(t)) - \mathcal{G}_1(t, W_2(t))|\right\}\right\}\right\}\right\} \\ &\leq L_{\mathcal{G}_1}\|W_1 - W_2\|_{\mathbb{X}}\frac{\beta T^{\alpha+\beta-1}}{(\alpha+\beta-1)\Gamma(\alpha)}. \end{aligned}$$

Then,

$$\|Q_1W_1 - Q_1W_2\|_{\mathbb{X}} \leq \frac{\beta T^{\alpha+\beta-1}L_{\mathcal{G}_1}}{(\alpha+\beta-1)\Gamma(\alpha)}\|W_1 - W_2\|_{\mathbb{X}}.$$

In the same way, we obtain that

$$\|Q_2M_1 - Q_2M_2\|_{\mathbb{X}} \leq \frac{\beta T^{\alpha+\beta-1}L_{\mathcal{G}_2}}{(\alpha+\beta-1)\Gamma(\alpha)}\|M_1 - M_2\|_{\mathbb{X}}, \ \ \|Q_3R_1 - Q_3R_2\|_{\mathbb{X}} \leq \frac{\beta T^{\alpha+\beta-1}L_{\mathcal{G}_3}}{(\alpha+\beta-1)\Gamma(\alpha)}\|R_1 - R_2\|_{\mathbb{X}}.$$

Since $Q = (Q_1, Q_2, Q_3)$ and $L_{\mathcal{G}}^{\max} = \max\{L_{\mathcal{G}_1}, L_{\mathcal{G}_2}, L_{\mathcal{G}_3}\} > 0$, we have

$$\|Q(W_1, M_1, R_1) - Q(W_2, M_2, R_2)\|_{\mathbb{X}} \leq \frac{\beta T^{\alpha+\beta-1}L_{\mathcal{G}_3}}{(\alpha+\beta-1)\Gamma(\alpha)}\|\mathbb{U}_1(t) - \mathbb{U}_2(t)\|_{\mathbb{X}}.$$

Under the inequality $\beta T^{\alpha+\beta-1}L_{\mathcal{G}}^{\max} < (\alpha+\beta-1)\Gamma(\alpha)$, we can summarize that Q is a contraction. Then, Q has a fixed point. Hence, the FFP-WPO model (2.16) has a unique solution. □

4.2. Ulam's stability results

Now, we give some sufficient criteria of the Ulam stability for the FFP-WPO model (2.16). The definitions of these types and some necessary remarks are given below.

Definition 4.2. *The FFP-WPO model* (2.16) *is said to be UH stable if there are positive numbers* $\epsilon_i > 0$, $(i = 1, 2, 3)$ *such that, for every* $\kappa_i > 0$, $(i = 1, 2, 3)$, *and each solution* $(W^*, M^*, R^*) \in \mathbb{X}$ *satisfying*

$$\left|{}_0^{FFP}\mathfrak{D}_t^{\alpha,\beta}W^*(t) - \mathcal{G}_1(t, W^*(t))\right| \leq \kappa_1, \quad t \in [0, T], \tag{4.9}$$

$$\left|{}_0^{FFP}\mathfrak{D}_t^{\alpha,\beta}M^*(t) - \mathcal{G}_2(t, M^*(t))\right| \leq \kappa_2, \quad t \in [0, T], \tag{4.10}$$

$$\left|{}_0^{FFP}\mathfrak{D}_t^{\alpha,\beta}R^*(t) - \mathcal{G}_3(t, R^*(t))\right| \leq \kappa_3, \quad t \in [0, T], \tag{4.11}$$

there is a solution $(W, M, R) \in \mathbb{X}$ *of the FFP-WPO model* (2.16) *under*

$$\|W(t) - W^*(t)\|_{\mathbb{X}} \leq \epsilon_1\kappa_1, \quad t \in [0, T], \tag{4.12}$$

$$\|M(t) - M^*(t)\|_{\mathbb{X}} \leq \epsilon_2\kappa_2, \quad t \in [0, T], \tag{4.13}$$

$$\|R(t) - R^*(t)\|_{\mathbb{X}} \leq \epsilon_3\kappa_3, \quad t \in [0, T], \tag{4.14}$$

where $\mathcal{G}_i(t, \cdot)$ *for* $i = 1, 2, 3$, *are given by* (4.2).

Definition 4.3. *The FFP-WPO model* (2.16) *is said to be GUH stable if there are functions* $\Xi_i(t) \in C(\mathbb{R}^+, \mathbb{R}^+)$*, with* $\Xi_i(0) = 0$*,* $(i = 1, 2, 3)$*, such that for every* $\kappa_i > 0$*,* $(i = 1, 2, 3)$*, and for each solution* $(W^*, M^*, R^*) \in \mathbb{X}$ *satisfying*

$$\begin{aligned} \left|{}_0^{FFP}\mathfrak{D}_t^{\alpha,\beta} W^*(t) - \mathcal{G}_1(t, W^*(t))\right| &\leq \kappa_1 \Xi_1(t), \quad t \in [0, T], \quad (4.15)\\ \left|{}_0^{FFP}\mathfrak{D}_t^{\alpha,\beta} M^*(t) - \mathcal{G}_2(t, M^*(t))\right| &\leq \kappa_2 \Xi_2(t), \quad t \in [0, T], \quad (4.16)\\ \left|{}_0^{FFP}\mathfrak{D}_t^{\alpha,\beta} R^*(t) - \mathcal{G}_3(t, R^*(t))\right| &\leq \kappa_3 \Xi_3(t), \quad t \in [0, T], \quad (4.17) \end{aligned}$$

there is a solution $(W, M, R) \in \mathbb{X}$ *of the FFP-WPO model* (2.16) *under*

$$\begin{aligned} \|W(t) - W^*(t)\|_{\mathbb{X}} &\leq \Xi_1(\kappa_1), \quad t \in [0, T], \quad (4.18)\\ \|M(t) - M^*(t)\|_{\mathbb{X}} &\leq \Xi_2(\kappa_2), \quad t \in [0, T], \quad (4.19)\\ \|R(t) - R^*(t)\|_{\mathbb{X}} &\leq \Xi_3(\kappa_3), \quad t \in [0, T], \quad (4.20) \end{aligned}$$

where $\mathcal{G}_i(t, \cdot)$*,* $i = 1, 2, 3$*, are given by* (4.2)*.*

Definition 4.4. *The FFP-WPO model* (2.16) *is said to be UHR stable with respect to* $\Xi_i(t) \in C([0, T], \mathbb{R}^+)$ *if there exist constants* $\Lambda_i \in \mathbb{R}^+$*,* $(i = 1, 2, 3)$*, such that for every* $\kappa_i > 0$*,* $(i = 1, 2, 3)$*, and for each solution* $(W^*, M^*, R^*) \in \mathbb{X}$ *satisfying inequalities* (4.15)–(4.17)*, respectively, there is a solution* $(W, M, R) \in \mathbb{X}$ *of the FFP-WPO model* (2.16) *under*

$$\begin{aligned} \|W(t) - W^*(t)\|_{\mathbb{X}} &\leq \Lambda_1\kappa_1 \Xi_1(t), \quad t \in [0, T], \quad (4.21)\\ \|M(t) - M^*(t)\|_{\mathbb{X}} &\leq \Lambda_2\kappa_2 \Xi_2(t), \quad t \in [0, T], \quad (4.22)\\ \|R(t) - R^*(t)\|_{\mathbb{X}} &\leq \Lambda_3\kappa_3 \Xi_3(t), \quad t \in [0, T], \quad (4.23) \end{aligned}$$

where $\mathcal{G}_i(t, \cdot)$*,* $i = 1, 2, 3$*, are given by* (4.2)*.*

Definition 4.5. *The FFP-WPO model* (2.16) *is said to be GUHR stable with respect to* $\Xi_i(t) \in C([0, T], \mathbb{R}^+)$ *if there exist constants* $\Lambda_i \in \mathbb{R}^+$*,* $(i = 1, 2, 3)$*, such that for each solution* $(W^*, M^*, R^*) \in \mathbb{X}$ *satisfying*

$$\begin{aligned} \left|{}_0^{FFP}\mathfrak{D}_t^{\alpha,\beta} W^*(t) - \mathcal{G}_1(t, W^*(t))\right| &\leq \Xi_1(t), \quad t \in [0, T], \quad (4.24)\\ \left|{}_0^{FFP}\mathfrak{D}_t^{\alpha,\beta} M^*(t) - \mathcal{G}_2(t, M^*(t))\right| &\leq \Xi_2(t), \quad t \in [0, T], \quad (4.25)\\ \left|{}_0^{FFP}\mathfrak{D}_t^{\alpha,\beta} R^*(t) - \mathcal{G}_3(t, R^*(t))\right| &\leq \Xi_3(t), \quad t \in [0, T], \quad (4.26) \end{aligned}$$

there is a solution $(W, M, R) \in \mathbb{X}$ *of the FFP-WPO model* (2.16) *under*

$$\begin{aligned} \|W(t) - W^*(t)\|_{\mathbb{X}} &\leq \Lambda_1 \Xi_1(t), \quad t \in [0, T], \quad (4.27)\\ \|M(t) - M^*(t)\|_{\mathbb{X}} &\leq \Lambda_2 \Xi_2(t), \quad t \in [0, T], \quad (4.28)\\ \|R(t) - R^*(t)\|_{\mathbb{X}} &\leq \Lambda_3 \Xi_3(t), \quad t \in [0, T], \quad (4.29) \end{aligned}$$

where $\mathcal{G}_i(t, \cdot)$ *for* $i = 1, 2, 3$*, are given by* (4.2)*.*

Remark 4.6. *Let* W^**,* M^**,* $R^* \in \mathbb{X}$ *be the solutions of inequalities* (4.9)–(4.11)*, respectively, if and only if there exists* $\chi_W(0) = 0$*,* $\chi_M(0) = 0$*, and* $\chi_R(0) = 0$ *satisfying*

(*i*) $|\chi_W(t)| \leq \kappa_1$, $|\chi_M(t)| \leq \kappa_2$, $|\chi_R(t)| \leq \kappa_3$;
(*ii*) ${}_0^{FFP}\mathfrak{D}_t^{\alpha,\beta} W^*(t) = \mathcal{G}_1(t, W^*(t)) + \chi_W(t)$, ${}_0^{FFP}\mathfrak{D}_t^{\alpha,\beta} M^*(t) = \mathcal{G}_2(t, M^*(t)) + \chi_M(t)$, ${}_0^{FFP}\mathfrak{D}_t^{\alpha,\beta} R^*(t) = \mathcal{G}_3(t, R^*(t)) + \chi_R(t)$.

Remark 4.7. *Let W^*, M^*, $R^* \in \mathbb{X}$ be the solutions of inequalities* (4.15)–(4.17)*, respectively, if and only if there exists $\phi_W(0) = 0$, $\phi_M(0) = 0$, and $\phi_R(0) = 0$ satisfying*

(*i*) $|\phi_W(t)| \leq \kappa_1 \Xi_1(t)$, $|\phi_M(t)| \leq \kappa_2 \Xi_2(t)$, $|\phi_R(t)| \leq \kappa_3 \Xi_3(t)$;
(*ii*) ${}_0^{FFP}\mathfrak{D}_t^{\alpha,\beta} W^*(t) = \mathcal{G}_1(t, W^*(t)) + \phi_W(t)$, ${}_0^{FFP}\mathfrak{D}_t^{\alpha,\beta} M^*(t) = \mathcal{G}_2(t, M^*(t)) + \phi_M(t)$, ${}_0^{FFP}\mathfrak{D}_t^{\alpha,\beta} R^*(t) = \mathcal{G}_3(t, R^*(t)) + \phi_R(t)$.

Theorem 4.8. *If all assumptions in Theorem 4.1 hold, then the FFP-WPO model* (2.16) *is UH stable as well as GUH stable.*

Proof. Suppose that $W^* \in \mathbb{X}$ is a solution of (4.9) and $\kappa_1 \in \mathbb{R}^+$. By applying Remark 4.6, we get

$$\begin{cases} {}_0^{FFP}\mathfrak{D}_t^{\alpha,\beta} W^*(t) = \mathcal{G}_1(t, W^*(t)) + \chi_W(t), \\ W^*(0) = W_0^* \geq 0. \end{cases} \tag{4.30}$$

So, the solution to (4.30) is provided as follows:

$$W^*(t) = W_0^* + \mathcal{L}_\beta^{-1}\left\{\frac{\beta}{s}\mathcal{L}_\beta\left\{\mathcal{L}^{-1}\left\{s^{1-\alpha}\mathcal{L}\left\{\mathcal{G}_1(t, W^*(t))\right\}\right\}\right\}\right\} + \mathcal{L}_\beta^{-1}\left\{\frac{\beta}{s}\mathcal{L}_\beta\left\{\mathcal{L}^{-1}\left\{s^{1-\alpha}\mathcal{L}\left\{\chi_W(t)\right\}\right\}\right\}\right\}.$$

Let $W \in \mathbb{X}$ be a unique solution of the FFP-WPO model (2.16). Then,

$$W(t) = W_0 + \mathcal{L}_\beta^{-1}\left\{\frac{\beta}{s}\mathcal{L}_\beta\left\{\mathcal{L}^{-1}\left\{s^{1-\alpha}\mathcal{L}\left\{\mathcal{G}_1(t, W(t))\right\}\right\}\right\}\right\}.$$

Hence,

$$\begin{aligned} \left|W^*(t) - W_0^* - \mathcal{L}_\beta^{-1}\left\{\frac{\beta}{s}\mathcal{L}_\beta\left\{\mathcal{L}^{-1}\left\{s^{1-\alpha}\mathcal{L}\left\{\mathcal{G}_1(t, W^*(t))\right\}\right\}\right\}\right\}\right| &\leq \beta\mathcal{L}_\beta^{-1}\left\{\frac{1}{s}\mathcal{L}_\beta\left\{\mathcal{L}^{-1}\left\{s^{1-\alpha}\mathcal{L}\left\{|\chi_W(t)|\right\}\right\}\right\}\right\} \\ &\leq \kappa_1\beta\mathcal{L}_\beta^{-1}\left\{\frac{1}{s}\mathcal{L}_\beta\left\{\mathcal{L}^{-1}\left\{s^{1-\alpha}\mathcal{L}\left\{1\right\}\right\}\right\}\right\} \\ &\leq \frac{\beta T^{\alpha+\beta-1}\kappa_1}{(\alpha+\beta-1)\Gamma(\alpha)}. \end{aligned} \tag{4.31}$$

Under the condition in Theorem 4.1 and inequality (4.31), one has

$$\begin{aligned} |W^*(t) - W(t)| &\leq \left|W^*(t) - W_0 - \mathcal{L}_\beta^{-1}\left\{\frac{\beta}{s}\mathcal{L}_\beta\left\{\mathcal{L}^{-1}\left\{s^{1-\alpha}\mathcal{L}\left\{\mathcal{G}_1(t, W(t))\right\}\right\}\right\}\right\}\right| \\ &\leq \left|W^*(t) - W_0^* - \mathcal{L}_\beta^{-1}\left\{\frac{\beta}{s}\mathcal{L}_\beta\left\{\mathcal{L}^{-1}\left\{s^{1-\alpha}\mathcal{L}\left\{\mathcal{G}_1(t, W^*(t))\right\}\right\}\right\}\right\}\right| \\ &\quad +\beta\mathcal{L}_\beta^{-1}\left\{\frac{1}{s}\mathcal{L}_\beta\left\{\mathcal{L}^{-1}\left\{s^{1-\alpha}\mathcal{L}\left\{|\mathcal{G}_1(t, W^*(t)) - \mathcal{G}_1(t, W(t))|\right\}\right\}\right\}\right\} \\ &\leq \frac{\beta T^{\alpha+\beta-1}}{(\alpha+\beta-1)\Gamma(\alpha)}\left(\kappa_1 + \mathcal{L}_{\mathcal{G}_1}|W^*(t) - W(t)|\right). \end{aligned}$$

Then,

$$\|W^* - W\|_{\mathbb{X}} \leq \frac{\beta T^{\alpha+\beta-1}\kappa_1}{(\alpha+\beta-1)\Gamma(\alpha)}\left(1 - \frac{\beta T^{\alpha+\beta-1}\mathcal{L}_{\mathcal{G}_1}}{(\alpha+\beta-1)\Gamma(\alpha)}\right)^{-1}.$$

Taking a constant

$$\epsilon_1 := \frac{\beta T^{\alpha+\beta-1}}{(\alpha+\beta-1)\Gamma(\alpha)}\left(1 - \frac{\beta T^{\alpha+\beta-1}\mathcal{L}_{\mathcal{G}_1}}{(\alpha+\beta-1)\Gamma(\alpha)}\right)^{-1},$$

yields that $\|W^* - W\|_{\mathbb{X}} \leq \epsilon_1\kappa_1$. In the same way, we obtain

$$\|M^* - M\|_{\mathbb{X}} \leq \epsilon_2\kappa_2 \quad \text{and} \quad \|R^* - R\|_{\mathbb{X}} \leq \epsilon_3\kappa_3,$$

where

$$\epsilon_i := \frac{\beta T^{\alpha+\beta-1}}{(\alpha+\beta-1)\Gamma(\alpha)}\left(1 - \frac{\beta T^{\alpha+\beta-1}\mathcal{L}_{\mathcal{G}_i}}{(\alpha+\beta-1)\Gamma(\alpha)}\right)^{-1}, \quad i = 2, 3.$$

Hence, by Definition 4.2, the FFP-WPO model (2.16) is UH stable. Additionally, by setting $\Xi_i(\kappa_i) = \epsilon_i\kappa_i$ with $\Xi_i(0) = 0$ for $i = 1, 2, 3$, by Definition 4.3, the FFP-WPO model (2.16) is GUH stable. □

Before proving this, we provide the following sufficient assumption:

($\mathcal{H}_2$) There are increasing functions $\Xi_i \in C([0, T], \mathbb{R}^+)$ and constants $\eta_i \in \mathbb{R}^+$, $i = 1, 2, 3$, such that for $t \in [0, T]$,

$$\mathcal{L}_\beta^{-1}\left\{\frac{\beta}{s}\mathcal{L}_\beta\left\{\mathcal{L}^{-1}\left\{s^{1-\alpha}\mathcal{L}\left\{\Xi_i(t)\right\}\right\}\right\}\right\} \leq \eta_i\Xi_i(t).$$

Theorem 4.9. *If all assumptions in Theorem 4.1 are satisfied and ($\mathcal{H}_2$) holds, then the FFP-WPO model* (2.16) *is UHR stable as well as GUHR stable.*

Proof. Suppose that $W^* \in \mathbb{X}$ is a solution of (4.15) and $\kappa_1 \in \mathbb{R}^+$. Applying Remark 4.6, yields

$$\begin{cases} {}_0^{FFP}\mathfrak{D}_t^{\alpha,\beta}W^*(t) = \mathcal{G}_1(t, W^*(t)) + \phi_W(t), \\ W^*(0) = W_0^* \geq 0. \end{cases} \tag{4.32}$$

Then, the solution to (4.32) is as follows:

$$W^*(t) = W_0^* + \beta\mathcal{L}_\beta^{-1}\left\{\frac{1}{s}\mathcal{L}_\beta\left\{\mathcal{L}^{-1}\left\{s^{1-\alpha}\mathcal{L}\left\{\mathcal{G}_1(t, W^*(t))\right\}\right\}\right\}\right\} + \beta\mathcal{L}_\beta^{-1}\left\{\frac{1}{s}\mathcal{L}_\beta\left\{\mathcal{L}^{-1}\left\{s^{1-\alpha}\mathcal{L}\left\{\phi_W(t)\right\}\right\}\right\}\right\}.$$

Let $W \in \mathbb{X}$ be a unique solution of the FFP-WPO model (2.16). Then,

$$W(t) = W_0 + \mathcal{L}_\beta^{-1}\left\{\frac{\beta}{s}\mathcal{L}_\beta\left\{\mathcal{L}^{-1}\left\{s^{1-\alpha}\mathcal{L}\left\{\mathcal{G}_1(t, W(t))\right\}\right\}\right\}\right\}.$$

Hence,

$$\begin{aligned} \left|W^*(t) - W_0^* - \mathcal{L}_\beta^{-1}\left\{\frac{\beta}{s}\mathcal{L}_\beta\left\{\mathcal{L}^{-1}\left\{s^{1-\alpha}\mathcal{L}\left\{\mathcal{G}_1(t, W^*(t))\right\}\right\}\right\}\right\}\right| &\leq \mathcal{L}_\beta^{-1}\left\{\frac{\beta}{s}\mathcal{L}_\beta\left\{\mathcal{L}^{-1}\left\{s^{1-\alpha}\mathcal{L}\left\{|\phi_W(t)|\right\}\right\}\right\}\right\} \\ &\leq \kappa_1\mathcal{L}_\beta^{-1}\left\{\frac{\beta}{s}\mathcal{L}_\beta\left\{\mathcal{L}^{-1}\left\{s^{1-\alpha}\mathcal{L}\left\{\Xi_1(t)\right\}\right\}\right\}\right\} \\ &\leq \kappa_1\eta_1\Xi_1(t). \end{aligned} \tag{4.33}$$

Under the condition in Theorem 4.1 and inequality (4.33), one has

$$\begin{aligned}
|W^*(t) - W(t)| &\leq \left| W^*(t) - W_0 - \mathcal{L}_\beta^{-1}\left\{\frac{\beta}{s}\mathcal{L}_\beta\left\{\mathcal{L}^{-1}\left\{s^{1-\alpha}\mathcal{L}\left\{\mathcal{G}_1(t, W(t))\right\}\right\}\right\}\right\}\right| \\
&\leq \left| W^*(t) - W_0^* - \mathcal{L}_\beta^{-1}\left\{\frac{\beta}{s}\mathcal{L}_\beta\left\{\mathcal{L}^{-1}\left\{s^{1-\alpha}\mathcal{L}\left\{\mathcal{G}_1(t, W^*(t))\right\}\right\}\right\}\right\}\right| \\
&\quad + \beta\mathcal{L}_\beta^{-1}\left\{\frac{1}{s}\mathcal{L}_\beta\left\{\mathcal{L}^{-1}\left\{s^{1-\alpha}\mathcal{L}\left\{|\mathcal{G}_1(t, W^*(t)) - \mathcal{G}_1(t, W(t))|\right\}\right\}\right\}\right\} \\
&\leq \kappa_1\eta_1\Xi_1(t) + \frac{\beta T^{\alpha+\beta-1}\mathcal{L}_{\mathcal{G}_1}}{(\alpha+\beta-1)\Gamma(\alpha)}\left|W^*(t) - W(t)\right|.
\end{aligned}$$

Then,

$$\|W^* - W\|_{\mathbb{X}} \leq \kappa_1\eta_1\Xi_1(t)\left(1 - \frac{\beta T^{\alpha+\beta-1}\mathcal{L}_{\mathcal{G}_1}}{(\alpha+\beta-1)\Gamma(\alpha)}\right)^{-1}.$$

Taking a constant

$$\Lambda_1 := \eta_1\left(1 - \frac{\beta T^{\alpha+\beta-1}\mathcal{L}_{\mathcal{G}_1}}{(\alpha+\beta-1)\Gamma(\alpha)}\right)^{-1}$$

yields that $\|W^* - W\|_{\mathbb{X}} \leq \Lambda_1\kappa_1\Xi_1$. In the same way, we obtain

$$\|M^* - M\|_{\mathbb{X}} \leq \Lambda_2\kappa_2\Xi_2 \quad \text{and} \quad \|R^* - R\|_{\mathbb{X}} \leq \Lambda_3\kappa_3\Xi_3,$$

where

$$\Lambda_i := \eta_i\left(1 - \frac{\beta T^{\alpha+\beta-1}\mathcal{L}_{\mathcal{G}_i}}{(\alpha+\beta-1)\Gamma(\alpha)}\right)^{-1}, \quad i = 2, 3.$$

Hence, by Definition 4.4, the FFP-WPO model (2.16) is UHR stable. Additionally, by setting $\Xi_i(t) = \kappa_i\Xi_i(t)$ with $\Xi_i(0) = 0$ for $i = 1, 2, 3$, by Definition 4.5, the FFP-WPO model (2.16) is GUHR stable. □

5. Numerical algorithms

5.1. Numerical method based on the decomposition technique

This section derives the numerical schemes for finding the approximate solution of the FFP-WPO model (2.16) by applying the decomposition formula for the FFP derivative operator. We will proceed in the same way as in [32, 33]. We show that the fractal-fractional Caputo derivative can be approximated using just the first-order derivative of a function $x(t)$. We can consider a system of $N + 1$ ordinary differential equations with the initial conditions of $N + 1$ conditions. A sequence (x_N), for $N \in \mathbb{N}$, of the solutions will converge to the solution of the fractal-fractional Caputo problem. The advantage of this technique is that, by replacing the fractal-fractional derivative with the expansion that only uses ordinary derivatives, we no longer have a fractal-fractional differential equation, but rather a system of ordinary differential equations. The solution to this system, x_N, clearly depends on N. However, the sequence x_N converges to the solution of the system of the fractal-fractional differential equations in a neighborhood of the initial point.

Theorem 5.1. *Assume that N is a positive number and $f \in AC^2([a,T],\mathbb{R})$. Let*

$$A_N = \sum_{i=0}^{N} \frac{\Gamma(i+\alpha-1)}{\Gamma(2-\alpha)\Gamma(\alpha-1)\,i!}, \qquad B_{N,i} = \frac{\Gamma(i+\alpha-1)}{\Gamma(2-\alpha)\Gamma(\alpha-1)\,(i-1)!}, \tag{5.1}$$

and $\mathcal{V}_i : [a,T] \to \mathbb{R}$ be functions defined by

$$\mathcal{V}_i(t) = \int_a^t \frac{(s-a)^{i-1}s^{1-\beta}}{\beta} f'(s)ds. \tag{5.2}$$

Then,

$$\begin{aligned} {}_0^{FFP_C}\mathfrak{D}_t^{\alpha,\beta}x(t) &= \mathcal{E}_N(t) + \frac{A_N t^{1-\beta}(t-a)^{1-\alpha}}{\beta} f'(t) \\ &\quad - \frac{1}{\Gamma(2-\alpha)} \sum_{i=1}^{N} B_{N,i}(t-a)^{1-\alpha-i}\mathcal{V}_i(t), \end{aligned} \tag{5.3}$$

where $\lim_{N\to\infty} \mathcal{E}_N(\tau) = 0$ *for* $t \in [a,T]$.

Proof. By applying Definition 2.4 for $\alpha \in (0,1]$, we obtain that

$${}_0^{FFP_C}\mathfrak{D}_t^{\alpha,\beta}x(t) = \frac{1}{\Gamma(1-\alpha)} \int_a^t (t-s)^{-\alpha} \frac{dx(s)}{ds^\beta} ds. \tag{5.4}$$

Let $u = \dfrac{dx(s)}{ds^\beta}$ and $dv = (t-s)^{-\alpha}ds$. Using the integration by parts method, yields that

$${}_0^{FFP_C}\mathfrak{D}_t^{\alpha,\beta}x(t) = \frac{a^{1-\beta}(t-a)^{1-\alpha}f'(a)}{\beta\Gamma(2-\alpha)} + \frac{1}{\Gamma(2-\alpha)} \int_a^t (t-s)^{-\alpha+1} \frac{d}{ds}\left[\frac{dx(s)}{ds^\beta}\right] ds. \tag{5.5}$$

Applying the generalized binomial theorem, it follows that

$$\begin{aligned} (t-s)^{1-\alpha} &= (t-a)^{1-\alpha}\left(1 - \frac{s-a}{t-a}\right)^{1-\alpha} \\ &= (t-a)^{1-\alpha} \sum_{i=0}^{\infty} \frac{\Gamma(i+\alpha-1)}{\Gamma(\alpha-1)\,i!}\left(\frac{s-a}{t-a}\right)^i. \end{aligned} \tag{5.6}$$

Plugging (5.6) into (5.5), it follows that

$$\begin{aligned} {}_0^{FFP_C}\mathfrak{D}_t^{\alpha,\beta}x(t) &= \mathcal{E}_N(t) + \frac{a^{1-\beta}(t-a)^{1-\alpha}f'(a)}{\beta\Gamma(2-\alpha)} \\ &\quad + \frac{1}{\Gamma(2-\alpha)} \int_a^t (t-a)^{1-\alpha} \sum_{i=0}^{N} \frac{\Gamma(i+\alpha-1)}{\Gamma(\alpha-1)\,i!}\left(\frac{s-a}{t-a}\right)^i \frac{d}{ds}\left[\frac{dx(s)}{ds^\beta}\right] ds, \end{aligned}$$

where

$$\mathcal{E}_N(t) = \frac{1}{\Gamma(2-\alpha)} \int_a^t (t-a)^{1-\alpha} \sum_{i=N+1}^{\infty} \frac{\Gamma(i+\alpha-1)}{\Gamma(\alpha-1)\,i!}\left(\frac{s-a}{t-a}\right)^i \frac{d}{ds}\left[\frac{dx(s)}{ds^\beta}\right] ds.$$

Hence, by direct calculation, we get

$$
\begin{aligned}
&{}_{0}^{FFP_C}\mathfrak{D}_t^{\alpha,\beta}x(t)\\
&= \mathcal{E}_N(t) + \frac{a^{1-\beta}(t-a)^{1-\alpha}f'(a)}{\beta\Gamma(2-\alpha)} + \frac{(t-a)^{1-\alpha}}{\Gamma(2-\alpha)}\sum_{i=0}^{N}\frac{\Gamma(i+\alpha-1)}{\Gamma(\alpha-1)\,i!(t-a)^i}\int_a^t (s-a)^i\frac{d}{ds}\left[\frac{dx(s)}{ds^\beta}\right]ds\\
&= \mathcal{E}_N(t) + \frac{a^{1-\beta}(t-a)^{1-\alpha}f'(a)}{\beta\Gamma(2-\alpha)} + \frac{(t-a)^{1-\alpha}}{\Gamma(2-\alpha)}\int_a^t \frac{d}{ds}\left[\frac{dx(s)}{ds^\beta}\right]ds\\
&\quad + \frac{(t-a)^{1-\alpha}}{\Gamma(2-\alpha)}\sum_{i=1}^{N}\frac{\Gamma(i+\alpha-1)}{\Gamma(\alpha-1)\,i!(t-a)^i}\int_a^t (s-a)^i\frac{d}{ds}\left[\frac{dx(s)}{ds^\beta}\right]ds\\
&= \mathcal{E}_N(t) + \frac{t^{1-\beta}(t-a)^{1-\alpha}f'(t)}{\beta\Gamma(2-\alpha)} + \frac{(t-a)^{1-\alpha}}{\Gamma(2-\alpha)}\sum_{i=1}^{N}\frac{\Gamma(i+\alpha-1)}{\Gamma(\alpha-1)\,i!(t-a)^i}\int_a^t (s-a)^i\frac{d}{ds}\left[\frac{dx(s)}{ds^\beta}\right]ds.
\end{aligned}
$$

Let $u = (s-a)^i$ and $dv = \frac{d}{ds}\left[\frac{dx(s)}{ds^\beta}\right]ds$. Using the integration by parts method, it follows that

$$
\begin{aligned}
{}_{0}^{FFP_C}\mathfrak{D}_t^{\alpha,\beta}x(t) &= \mathcal{E}_N(t) + \frac{t^{1-\beta}(t-a)^{1-\alpha}f'(t)}{\beta\Gamma(2-\alpha)} + \frac{(t-a)^{1-\alpha}}{\Gamma(2-\alpha)}\sum_{i=1}^{N}\frac{\Gamma(i+\alpha-1)}{\Gamma(\alpha-1)\,i!(t-a)^i}\frac{t^{1-\beta}(t-a)^i f'(t)}{\beta}\\
&\quad -\frac{(t-a)^{1-\alpha}}{\Gamma(2-\alpha)}\sum_{i=1}^{N}\frac{\Gamma(i+\alpha-1)}{\Gamma(\alpha-1)\,i!(t-a)^i}\int_a^t i(s-a)^{i-1}\frac{dx(s)}{ds^\beta}ds\\
&= \mathcal{E}_N(t) + \left[1+\sum_{i=1}^{N}\frac{\Gamma(i+\alpha-1)}{\Gamma(\alpha-1)\,i!}\right]\frac{t^{1-\beta}(t-a)^{1-\alpha}f'(t)}{\beta\Gamma(2-\alpha)}\\
&\quad -\frac{(t-a)^{1-\alpha}}{\Gamma(2-\alpha)}\sum_{i=1}^{N}\frac{\Gamma(i+\alpha-1)}{\Gamma(\alpha-1)\,i!(t-a)^i}\int_a^t \frac{i(s-a)^{i-1}s^{1-\beta}}{\beta}\frac{dx(s)}{ds}ds.
\end{aligned}
$$

Since $\Gamma(x+\alpha)\sim\Gamma(x)x^\alpha$ and $s/t<1$,

$$
\sum_{i=N+1}^{\infty}\frac{\Gamma(i+\alpha-1)}{i!}\left(\frac{s}{t}\right)^i \le \sum_{i=N+1}^{\infty}\frac{\Gamma(i+\alpha-1)}{i!} \le \sum_{i=N+1}^{\infty} i^{\alpha-2} \le \int_N^{\infty} s^{\alpha-2}ds \le \frac{N^{\alpha-1}}{1-\alpha}. \tag{5.7}
$$

Then, the right side of the above inequality (5.7) tends to zero for all $t\in(0,T)$ as $N\to\infty$. □

Next, we will utilize Theorem 5.1 to achieve the approximate solution of the FFP-WPO model (2.16). Hence,

$$
\begin{aligned}
{}_{0}^{FFP_C}\mathfrak{D}_t^{\alpha,\beta}W(t) &= \frac{A_N t^{1-\beta}(t-a)^{1-\alpha}}{\beta}W'(t) - \frac{1}{\Gamma(2-\alpha)}\sum_{i=1}^{N}B_{N,i}(t-a)^{1-\alpha-i}\mathcal{V}_{W_i}(t),\\
{}_{0}^{FFP_C}\mathfrak{D}_t^{\alpha,\beta}M(t) &= \frac{A_N t^{1-\beta}(t-a)^{1-\alpha}}{\beta}M'(t) - \frac{1}{\Gamma(2-\alpha)}\sum_{i=1}^{N}B_{N,i}(t-a)^{1-\alpha-i}\mathcal{V}_{M_i}(t),\\
{}_{0}^{FFP_C}\mathfrak{D}_t^{\alpha,\beta}R(t) &= \frac{A_N t^{1-\beta}(t-a)^{1-\alpha}}{\beta}R'(t) - \frac{1}{\Gamma(2-\alpha)}\sum_{i=1}^{N}B_{N,i}(t-a)^{1-\alpha-i}\mathcal{V}_{R_i}(t),
\end{aligned} \tag{5.8}
$$

and

$$\begin{aligned}
\mathcal{V}_{W_i}(t) &= \frac{1}{\beta}\int_a^t (s-a)^{i-1}s^{1-\beta}W'(s)ds,\\
\mathcal{V}_{M_i}(t) &= \frac{1}{\beta}\int_a^t (s-a)^{i-1}s^{1-\beta}M'(s)ds,\\
\mathcal{V}_{R_i}(t) &= \frac{1}{\beta}\int_a^t (s-a)^{i-1}s^{1-\beta}R'(s)ds,
\end{aligned}$$

where A_N and $B_{N,i}$ are provided by (5.1).

5.2. Numerical method based on the Adams-Bashforth technique

The Adams-Bashforth method is a powerful numerical integration approach that is widely utilized to solve differential equations [34]. Its higher-order accuracy and efficiency make it especially well-suited for approximating dynamic system solutions. We used the Adams-Bashforth method to obtain accurate and reliable numerical solutions for the FFP-WPO model (2.16). By using Definition 2.1 in the FFP-WPO model (2.16), we have the following results:

$$W(t) = W_0 + \frac{\beta}{\Gamma(\alpha)}\int_0^t s^{\beta-1}(t-s)^{\alpha-1}\mathcal{G}_1(s,W)ds, \tag{5.9}$$

$$M(t) = M_0 + \frac{\beta}{\Gamma(\alpha)}\int_0^t s^{\beta-1}(t-s)^{\alpha-1}\mathcal{G}_2(s,M)ds, \tag{5.10}$$

$$R(t) = R_0 + \frac{\beta}{\Gamma(\alpha)}\int_0^t s^{\beta-1}(t-s)^{\alpha-1}\mathcal{G}_3(s,R)ds. \tag{5.11}$$

We rewrite (5.9)–(5.11) at $t = t_{n+1} = (n+1)h$ with $h = T/N$, which gives

$$W(t_{n+1}) = W_0 + \frac{\beta}{\Gamma(\alpha)}\int_0^{t_{n+1}} s^{\beta-1}(t_{n+1}-s)^{\alpha-1}\mathcal{G}_1(s,W)ds, \tag{5.12}$$

$$M(t_{n+1}) = M_0 + \frac{\beta}{\Gamma(\alpha)}\int_0^{t_{n+1}} s^{\beta-1}(t_{n+1}-s)^{\alpha-1}\mathcal{G}_2(s,M)ds, \tag{5.13}$$

$$R(t_{n+1}) = R_0 + \frac{\beta}{\Gamma(\alpha)}\int_0^{t_{n+1}} s^{\beta-1}(t_{n+1}-s)^{\alpha-1}\mathcal{G}_3(s,R)ds. \tag{5.14}$$

By using the approximation of the integrals in (5.12)–(5.14), we have that

$$W(t_{n+1}) = W_0 + \frac{\beta}{\Gamma(\alpha)}\sum_{j=1}^{n}\int_{t_j}^{t_{j+1}} s^{\beta-1}(t_{n+1}-s)^{\alpha-1}\mathcal{G}_1(s,W)ds, \tag{5.15}$$

$$M(t_{n+1}) = M_0 + \frac{\beta}{\Gamma(\alpha)} \sum_{j=1}^{n} \int_{t_j}^{t_{j+1}} s^{\beta-1}(t_{n+1}-s)^{\alpha-1} \mathcal{G}_2(s, M) ds, \tag{5.16}$$

$$R(t_{n+1}) = R_0 + \frac{\beta}{\Gamma(\alpha)} \sum_{j=1}^{n} \int_{t_j}^{t_{j+1}} s^{\beta-1}(t_{n+1}-s)^{\alpha-1} \mathcal{G}_3(s, R) ds. \tag{5.17}$$

Applying two-step Lagrange interpolation polynomials via $h = t_{j+1} - t_j$ for the term $s^{\beta-1}\mathcal{G}_1(s, W)$, yields

$$\mathbb{L}_j^W(s) = \frac{s-t_{j-1}}{h} t_j^{\beta-1} \mathcal{G}_1(t_j, W_j) - \frac{s-t_j}{h} t_{j-1}^{\beta-1} \mathcal{G}_1(t_{j-1}, W_{j-1}), \tag{5.18}$$

$$\mathbb{L}_j^M(s) = \frac{s-t_{j-1}}{h} t_j^{\beta-1} \mathcal{G}_2(t_j, M_j) - \frac{s-t_j}{h} t_{j-1}^{\beta-1} \mathcal{G}_2(t_{j-1}, M_{j-1}), \tag{5.19}$$

$$\mathbb{L}_j^R(s) = \frac{s-t_{j-1}}{h} t_j^{\beta-1} \mathcal{G}_3(t_j, R_j) - \frac{s-t_j}{h} t_{j-1}^{\beta-1} \mathcal{G}_3(t_{j-1}, R_{j-1}). \tag{5.20}$$

Plugging (5.18)–(5.20) into (5.15)–(5.17), we get

$$W(t_{n+1}) = W_0 + \frac{\beta h^\alpha}{\Gamma(\alpha+2)} \sum_{j=1}^{n} \left[\Phi_1(n, j) t_j^{\beta-1} \mathcal{G}_1(t_j, W_j) - \Phi_2(n, j) t_{j-1}^{\beta-1} \mathcal{G}_1(t_{j-1}, W_{j-1}) \right],$$

$$M(t_{n+1}) = M_0 + \frac{\beta h^\alpha}{\Gamma(\alpha+2)} \sum_{j=1}^{n} \left[\Phi_1(n, j) t_j^{\beta-1} \mathcal{G}_2(t_j, M_j) - \Phi_2(n, j) t_{j-1}^{\beta-1} \mathcal{G}_2(t_{j-1}, M_{j-1}) \right],$$

$$R(t_{n+1}) = R_0 + \frac{\beta h^\alpha}{\Gamma(\alpha+2)} \sum_{j=1}^{n} \left[\Phi_1(n, j) t_j^{\beta-1} \mathcal{G}_3(t_j, R_j) - \Phi_2(n, j) t_{j-1}^{\beta-1} \mathcal{G}_3(t_{j-1}, R_{j-1}) \right],$$

where $\Phi_1(n, j)$ and $\Phi_2(n, j)$ are provided by

$$\Phi_1(n, j) = (n+1-j)^\alpha (n-j+2+\alpha) - (n-j)^\alpha (n-j+2+2\alpha),$$
$$\Phi_2(n, j) = (n+1-j)^{\alpha+1} - (n-j)^\alpha (n-j+1+\alpha).$$

5.3. Numerical method based on the newton polynomial technique

We describe a Newton's polynomial-based approximation method for numerically calculating the solutions of the FFP-WPO model (2.16). Newton's polynomials are used in interpolation because they are implicit and useful for estimating functions based on a collection of provided data points. Newton's polynomials provide a versatile technique to describe complicated interactions inside the FFP-WPO model (2.16) when modeling and analyzing it. By using the polynomial interpolation approach, we may create a continuous function that roughly represents the system's behavior, allowing for a more thorough and in-depth comprehension of its dynamics. To the best of our knowledge, the concept was initially presented by Atangana and Araz in [35]. Using the approximation of the integrals in (5.12)–(5.14), we have that

$$W(t_{n+1}) = W_0 + \frac{\beta}{\Gamma(\alpha)} \sum_{j=2}^{n} \int_{t_j}^{t_{j+1}} s^{\beta-1}(t_{n+1}-s)^{\alpha-1} \mathcal{G}_1(s, W) ds, \tag{5.21}$$

$$M(t_{n+1}) = M_0 + \frac{\beta}{\Gamma(\alpha)} \sum_{j=2}^{n} \int_{t_j}^{t_{j+1}} s^{\beta-1}(t_{n+1}-s)^{\alpha-1}\mathcal{G}_2(s,M)ds, \tag{5.22}$$

$$R(t_{n+1}) = R_0 + \frac{\beta}{\Gamma(\alpha)} \sum_{j=2}^{n} \int_{t_j}^{t_{j+1}} s^{\beta-1}(t_{n+1}-s)^{\alpha-1}\mathcal{G}_3(s,R)ds. \tag{5.23}$$

Applying the newton polynomial for the term $s^{\beta-1}\mathcal{G}_1(s,W)$ yields

$$\begin{aligned}
\mathbb{P}_j^W(s) &= t_{j-2}^{\beta-1}\mathcal{G}_1(t_{j-2},W_{j-2}) + \frac{s-t_{j-2}}{h}\left[t_{j-1}^{\beta-1}\mathcal{G}_1(t_{j-1},W_{j-1}) - t_{j-2}^{\beta-1}\mathcal{G}_1(t_{j-2},W_{j-2})\right] \\
&\quad + \frac{(s-t_{j-1})(s-t_{j-2})}{2h^2}\left[t_j^{\beta-1}\mathcal{G}_1(t_j,W_j) - 2t_{j-1}^{\beta-1}\mathcal{G}_1(t_{j-1},W_{j-1}) + t_{j-2}^{\beta-1}\mathcal{G}_1(t_{j-2},W_{j-2})\right], \quad (5.24) \\
\mathbb{P}_j^M(s) &= t_{j-2}^{\beta-1}\mathcal{G}_2(t_{j-2},M_{j-2}) + \frac{s-t_{j-2}}{h}\left[t_{j-1}^{\beta-1}\mathcal{G}_2(t_{j-1},M_{j-1}) - t_{j-2}^{\beta-1}\mathcal{G}_2(t_{j-2},M_{j-2})\right] \\
&\quad + \frac{(s-t_{j-1})(s-t_{j-2})}{2h^2}\left[t_j^{\beta-1}\mathcal{G}_2(t_j,M_j) - 2t_{j-1}^{\beta-1}\mathcal{G}_2(t_{j-1},M_{j-1}) + t_{j-2}^{\beta-1}\mathcal{G}_2(t_{j-2},M_{j-2})\right], \quad (5.25) \\
\mathbb{P}_j^R(s) &= t_{j-2}^{\beta-1}\mathcal{G}_3(t_{j-2},R_{j-2}) + \frac{s-t_{j-2}}{h}\left[t_{j-1}^{\beta-1}\mathcal{G}_3(t_{j-1},R_{j-1}) - t_{j-2}^{\beta-1}\mathcal{G}_3(t_{j-2},R_{j-2})\right] \\
&\quad + \frac{(s-t_{j-1})(s-t_{j-2})}{2h^2}\left[t_j^{\beta-1}\mathcal{G}_3(t_j,R_j) - 2t_{j-1}^{\beta-1}\mathcal{G}_3(t_{j-1},R_{j-1}) + t_{j-2}^{\beta-1}\mathcal{G}_3(t_{j-2},R_{j-2})\right]. \quad (5.26)
\end{aligned}$$

Plugging (5.24)–(5.26) into (5.21)–(5.23), we get

$$\begin{aligned}
W(t_{n+1}) &= W_0 + \frac{\beta h^\alpha}{\Gamma(\alpha+1)}\sum_{j=2}^{n}\Omega_1(n,j)t_{j-2}^{\beta-1}\mathcal{G}_1(t_{j-2},W_{j-2}) \\
&\quad + \frac{\beta h^\alpha}{\Gamma(\alpha+2)}\sum_{j=2}^{n}\Omega_2(n,j)\left(t_{j-1}^{\beta-1}\mathcal{G}_1(t_{j-1},W_{j-1}) - t_{j-2}^{\beta-1}\mathcal{G}_1(t_{j-2},W_{j-2})\right) \\
&\quad + \frac{\beta h^\alpha}{2\Gamma(\alpha+3)}\sum_{j=2}^{n}\Omega_3(n,j)\left(t_j^{\beta-1}\mathcal{G}_1(t_j,W_j) - 2t_{j-1}^{\beta-1}\mathcal{G}_1(t_{j-1},W_{j-1}) + t_{j-2}^{\beta-1}\mathcal{G}_1(t_{j-2},W_{j-2})\right), \\
M(t_{n+1}) &= M_0 + \frac{\beta h^\alpha}{\Gamma(\alpha+1)}\sum_{j=2}^{n}\Omega_1(n,j)t_{j-2}^{\beta-1}\mathcal{G}_2(t_{j-2},M_{j-2}) \\
&\quad + \frac{\beta h^\alpha}{\Gamma(\alpha+2)}\sum_{j=2}^{n}\Omega_2(n,j)\left(t_{j-1}^{\beta-1}\mathcal{G}_2(t_{j-1},M_{j-1}) - t_{j-2}^{\beta-1}\mathcal{G}_2(t_{j-2},M_{j-2})\right) \\
&\quad + \frac{\beta h^\alpha}{2\Gamma(\alpha+3)}\sum_{j=2}^{n}\Omega_3(n,j)\left(t_j^{\beta-1}\mathcal{G}_2(t_j,M_j) - 2t_{j-1}^{\beta-1}\mathcal{G}_2(t_{j-1},M_{j-1}) + t_{j-2}^{\beta-1}\mathcal{G}_2(t_{j-2},M_{j-2})\right), \\
R(t_{n+1}) &= R_0 + \frac{\beta h^\alpha}{\Gamma(\alpha+1)}\sum_{j=2}^{n}\Omega_1(n,j)t_{j-2}^{\beta-1}\mathcal{G}_3(t_{j-2},R_{j-2}) \\
&\quad + \frac{\beta h^\alpha}{\Gamma(\alpha+2)}\sum_{j=2}^{n}\Omega_2(n,j)\left(t_{j-1}^{\beta-1}\mathcal{G}_3(t_{j-1},R_{j-1}) - t_{j-2}^{\beta-1}\mathcal{G}_3(t_{j-2},R_{j-2})\right)
\end{aligned}$$

$$+\frac{\beta h^{\alpha}}{2\Gamma(\alpha+3)}\sum_{j=2}^{n}\Omega_3(n,j)\Big(t_j^{\beta-1}\mathcal{G}_3(t_j,R_j)-2t_{j-1}^{\beta-1}\mathcal{G}_3(t_{j-1},R_{j-1})+t_{j-2}^{\beta-1}\mathcal{G}_3(t_{j-2},R_{j-2})\Big),$$

where $\Omega_1(n,j)$, $\Omega_2(n,j)$, and $\Omega_3(n,j)$ are given by

$$\begin{aligned}
\Omega_1(n,j) &= (n-j+1)^{\alpha}-(n-j)^{\alpha},\\
\Omega_2(n,j) &= (2\alpha-j+n+3)(n-j+1)^{\alpha}-(3\alpha-j+n+3)(n-j)^{\alpha},\\
\Omega_3(n,j) &= \Big[2(n-j)^2+(3\alpha+10)(n-j)+2\alpha^2+9\alpha+12\Big](n-j+1)^{\alpha}\\
&\quad-\Big[2(n-j)^2+(5\alpha+10)(n-j)+6\alpha^2+9\alpha+12\Big](n-j)^{\alpha}.
\end{aligned}$$

5.4. Numerical method based on the predictor-corrector technique

This part illustrates the numerical scheme for the FFP-WPO model (2.16), which was created using the predictor-corrector technique. It is among the most efficient, reliable, and accurate methods for numerically solving fractal-fractional differential equations in the Caputo sense. To build the predictor-corrector approach for the proposed problem, we will use the same procedure as in [36,37] with certain adjustments. Applying the approximation of the integrals in (5.12)–(5.14), we have that

$$W(t_{n+1}) = W_0+\frac{\beta}{\Gamma(\alpha)}\sum_{j=0}^{n}\int_{t_j}^{t_{j+1}}s^{\beta-1}(t_{n+1}-s)^{\alpha-1}\mathcal{G}_1(s,W)ds, \tag{5.27}$$

$$M(t_{n+1}) = M_0+\frac{\beta}{\Gamma(\alpha)}\sum_{j=0}^{n}\int_{t_j}^{t_{j+1}}s^{\beta-1}(t_{n+1}-s)^{\alpha-1}\mathcal{G}_2(s,M)ds, \tag{5.28}$$

$$R(t_{n+1}) = R_0+\frac{\beta}{\Gamma(\alpha)}\sum_{j=0}^{n}\int_{t_j}^{t_{j+1}}s^{\beta-1}(t_{n+1}-s)^{\alpha-1}\mathcal{G}_3(s,R)ds. \tag{5.29}$$

Approximating the function $s^{\beta-1}\mathcal{G}_1(s,W)$ by piece-wise linear interpolation gives

$$\mathbb{J}_j^W(s) = t_j^{\beta-1}\mathcal{G}_1(t_j,W_j)+\frac{t_{j+1}^{\beta-1}\mathcal{G}_1(t_{j+1},W_{j+1})-t_j^{\beta-1}\mathcal{G}_1(t_j,W_j)}{t_{j+1}-t_j}(s-t_j), \tag{5.30}$$

$$\mathbb{J}_j^M(s) = t_j^{\beta-1}\mathcal{G}_2(t_j,M_j)+\frac{t_{j+1}^{\beta-1}\mathcal{G}_2(t_{j+1},M_{j+1})-t_j^{\beta-1}\mathcal{G}_2(t_j,M_j)}{t_{j+1}-t_j}(s-t_j), \tag{5.31}$$

$$\mathbb{J}_j^R(s) = t_j^{\beta-1}\mathcal{G}_3(t_j,R_j)+\frac{t_{j+1}^{\beta-1}\mathcal{G}_3(t_{j+1},R_{j+1})-t_j^{\beta-1}\mathcal{G}_3(t_j,R_j)}{t_{j+1}-t_j}(s-t_j). \tag{5.32}$$

Plugging (5.30)–(5.32) into (5.27)–(5.29), we get

$$W_{n+1} = W_0+\frac{\beta h^{\alpha}}{\Gamma(\alpha+2)}\sum_{j=0}^{n}\Xi_1(n,j)t_j^{\beta-1}\mathcal{G}_1(t_j,W_j)+\frac{\beta h^{\alpha}}{\Gamma(\alpha+2)}t_{n+1}^{\beta-1}\mathcal{G}_1(t_{n+1},W_{n+1}^P), \tag{5.33}$$

$$M_{n+1} = M_0+\frac{\beta h^{\alpha}}{\Gamma(\alpha+2)}\sum_{j=0}^{n}\Xi_1(n,j)t_j^{\beta-1}\mathcal{G}_2(t_j,M_j)+\frac{\beta h^{\alpha}}{\Gamma(\alpha+2)}t_{n+1}^{\beta-1}\mathcal{G}_2(t_{n+1},M_{n+1}^P), \tag{5.34}$$

$$R_{n+1} = R_0 + \frac{\beta h^\alpha}{\Gamma(\alpha+2)}\sum_{j=0}^{n}\Xi_1(n,j)t_j^{\beta-1}\mathcal{G}_3(t_j,R_j) + \frac{\beta h^\alpha}{\Gamma(\alpha+2)}t_{n+1}^{\beta-1}\mathcal{G}_3(t_{n+1},R_{n+1}^P). \quad (5.35)$$

Repeating the above process for $W(t)$, $M(t)$, and $R(t)$, implies that

$$\begin{aligned}
W_{n+1}^P &= W_0 + \frac{\beta h^\alpha}{\Gamma(\alpha+1)}\sum_{j=0}^{n}\Xi_2(n,j)t_j^{\beta-1}\mathcal{G}_1(t_j,W_j),\\
M_{n+1}^P &= M_0 + \frac{\beta h^\alpha}{\Gamma(\alpha+1)}\sum_{j=0}^{n}\Xi_2(n,j)t_j^{\beta-1}\mathcal{G}_2(t_j,M_j),\\
R_{n+1}^P &= R_0 + \frac{\beta h^\alpha}{\Gamma(\alpha+1)}\sum_{j=0}^{n}\Xi_2(n,j)t_j^{\beta-1}\mathcal{G}_3(t_j,R_j),
\end{aligned}$$

where $\Xi_1(n,j)$ and $\Xi_2(n,j)$ are given by

$$\begin{aligned}
\Xi_1(n,j) &= \begin{cases} n^{\alpha+1} - (n-\alpha)(n+1)^\alpha, & if \quad j=0,\\ (n-j+2)^{\alpha+1} - 2(n-j+1)^{\alpha+1} + (n-j)^{\alpha+1}, & if \quad 0<j\le n, \end{cases}\\
\Xi_2(n,j) &= (n-j+1)^\alpha - (n-j)^\alpha.
\end{aligned}$$

6. Numerical simulations and discussion

This section presents the numerical simulations of the approximate solution for the FFP-WPO model (2.16) using the given numerical techniques in Section 5. By using a sensitivity analysis (Section 3.3) of the BRN (P_0), we now investigate the impact of each parameter on the dynamics of the FFP-WPO model (2.16). The parameter values utilized in the numerical simulations are used in [1, 2, 4] for the FFP-WPO model (2.16). The approximate solutions have been investigated for various fractional-orders, fractal-dimensions, and parameters.

6.1. Impact of the fractional-order derivative on the FFP-WPO model (2.16)

6.1.1. The marine debris-free equilibrium point $\mathfrak{E}_0^*$

Set $\alpha = 0.83, 0.87, 0.91, 0.95, 0.99$ and $\beta = 0.99$ with the given parameters $b = 0.15$, $a = 0.65$, $\Lambda = 0.36$, $\mu = 0.40$, $\gamma = 0.41$, and $\theta = 0.15$, and the initial conditions $(W_0, M_0, R_0) = (2, 1.5, 1)$. Then, Theorem 3.4 is satisfied. We expect that the marine debris-free equilibrium point $\mathfrak{E}_0^* = (W_0^*, M_0^*, R_0^*) = (3.2195, 0, 2.4)$ is GAS, which means that the solutions of the FFP-WPO model (2.16) should tend to the marine debris-free equilibrium point $\mathfrak{E}_0^*$. In Figures 3–5, the dynamical behavior of the management of waste plastic in the ocean is presented when $P_0 = 0.7430 < 1$. At this stage, the marine debris-free equilibrium ($\mathfrak{E}_0^*$) is such that the amount of marine debris is zero. Additionally, Figure 3 (Figure 3a– 3d) depicts the dynamical behavior of the waste plastic material $W(t)$. When α (fractional-order) grows from 0.83 to 0.99 and β (fractal-dimension) is 0.99, the process quickly increases from the start and finally converges to a stable state at the point $W_0^* \approx 3.2195$. Figure 4 (Figure 4a–4d) depicts the dynamical behavior of the marine debris $M(t)$. When α grows from 0.83 to 0.99 and $\beta = 0.99$, the process quickly decreases from the start and finally converges to a stable state at $M_0^* = 0$. Figure 5

(Figure 5a– 5d) depicts the dynamical behavior of the reprocessing or recycling $R(t)$. When α grows from 0.83 to 0.99 and $\beta = 0.99$, the process quickly increases from the start and finally converges to a stable state at $R_0^* = 2.4$.

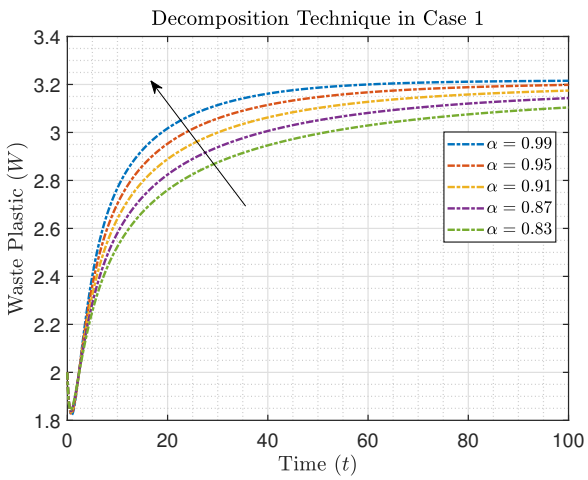

(a) Decomposition Technique

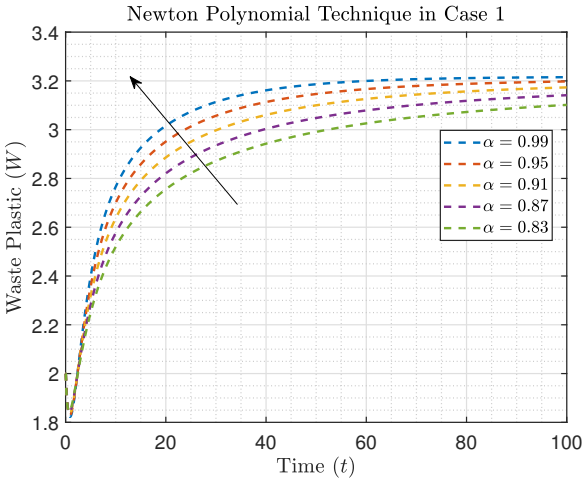

(b) Newton Polynomial Technique

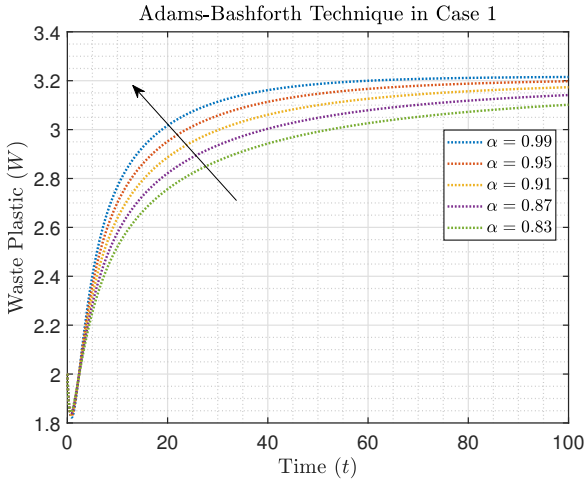

(c) Adam-Bashforth Technique

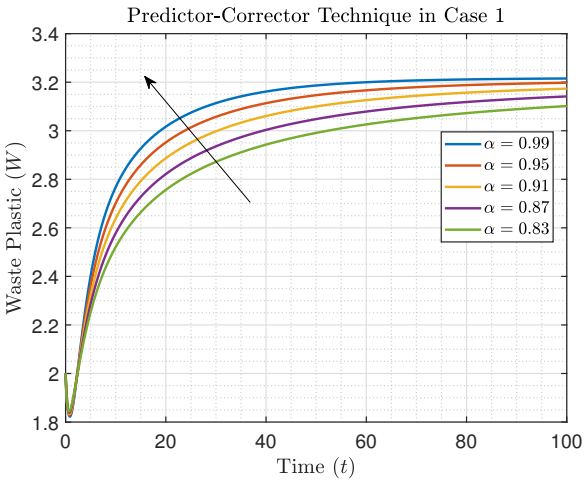

(d) Predictor-Corrector Technique

Figure 3. Numerical simulations of $W(t)$ for the FFP-WPO model (2.16) using four numerical techniques.

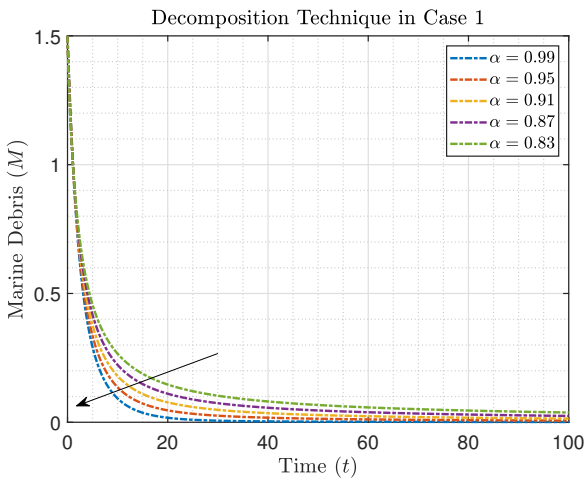

(a) Decomposition Technique

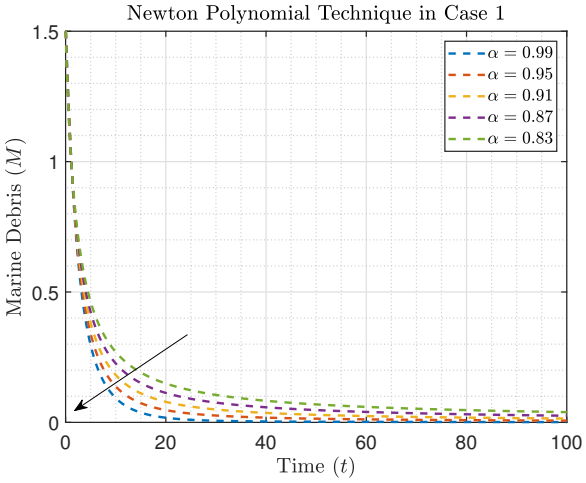

(b) Newton Polynomial Technique

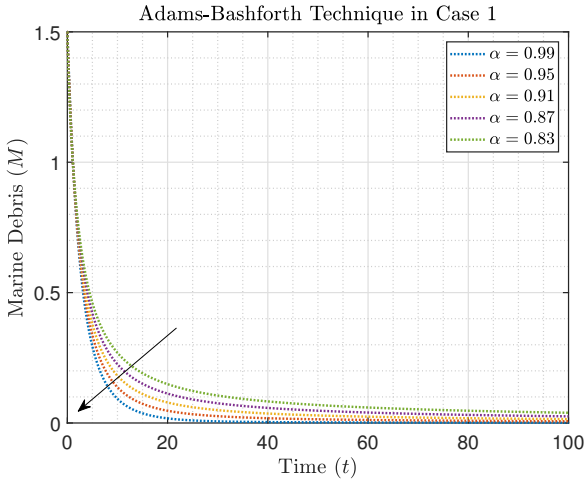

(c) Adam-Bashforth Technique

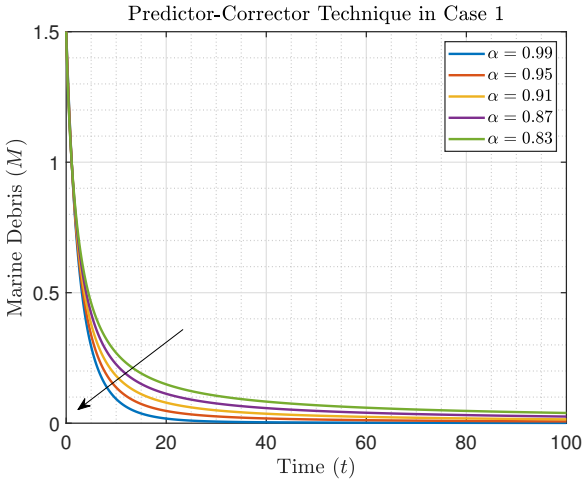

(d) Predictor-Corrector Technique

Figure 4. Numerical simulations of $M(t)$ for the FFP-WPO model (2.16) using four numerical techniques.

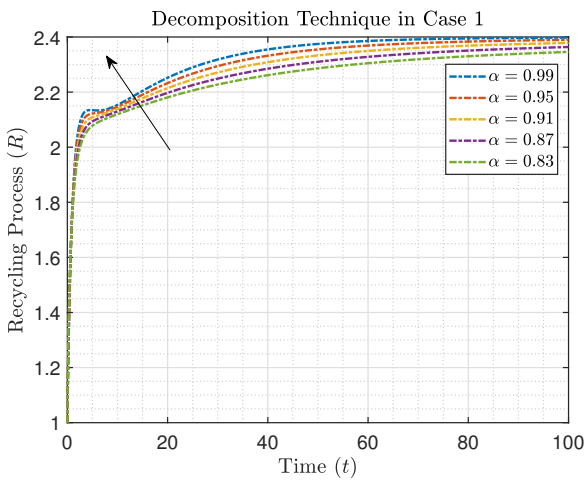

(a) Decomposition Technique

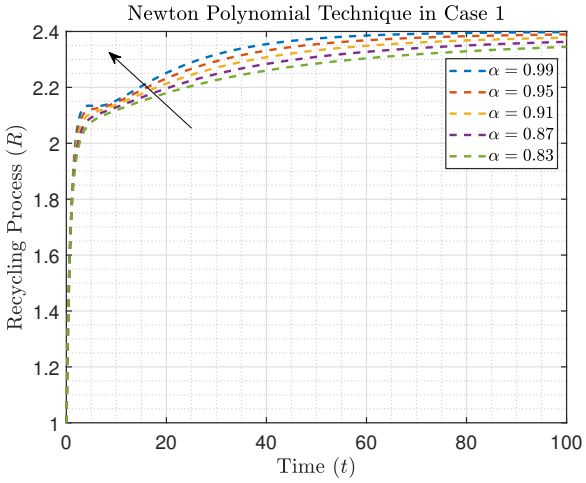

(b) Newton Polynomial Technique

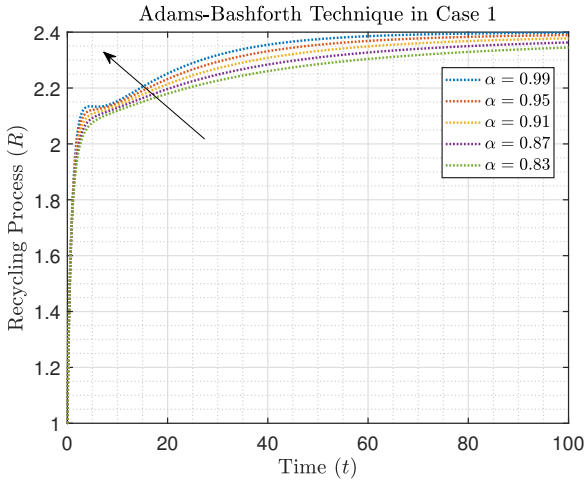

(c) Adam-Bashforth Technique

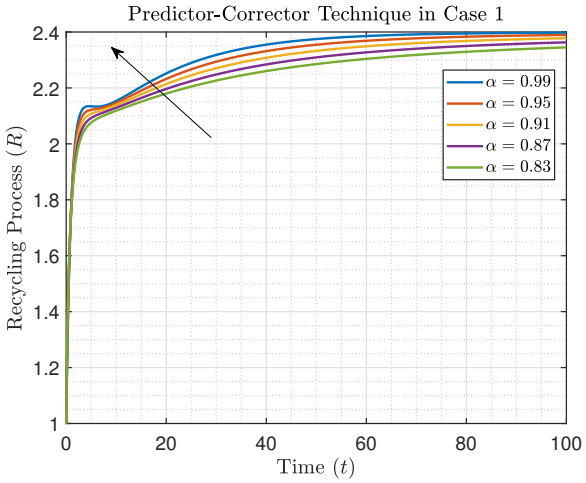

(d) Predictor-Corrector Technique

Figure 5. Numerical simulations of $R(t)$ for the FFP-WPO model (2.16) using four numerical techniques.

Using the four different numerical schemes, i.e., the decomposition, Newton polynomial, Adams-Bashforth, and predictor-corrector methods, Figure 6 illustrates comparisons of simulation results using four techniques for three compartments: waste plastic material $W(t)$ (Figure 6a), marine debris $M(t)$ (Figure 6b), and reprocessing or recycling $R(t)$ (Figure 6c) where $\alpha = \beta = 0.99$. To compare the results of the four numerical techniques for the three state compartments, we show some numerical results in Table 2. It can be observed that the graphical simulations and numerical results of these four numerical techniques are quite comparable with little difference. In addition, we also show a comparison of the results between the classical derivative, the fractional derivative, and the fractal-fractional derivative for the FFP-WPO model (2.16) in Figure 7 and Table 3.

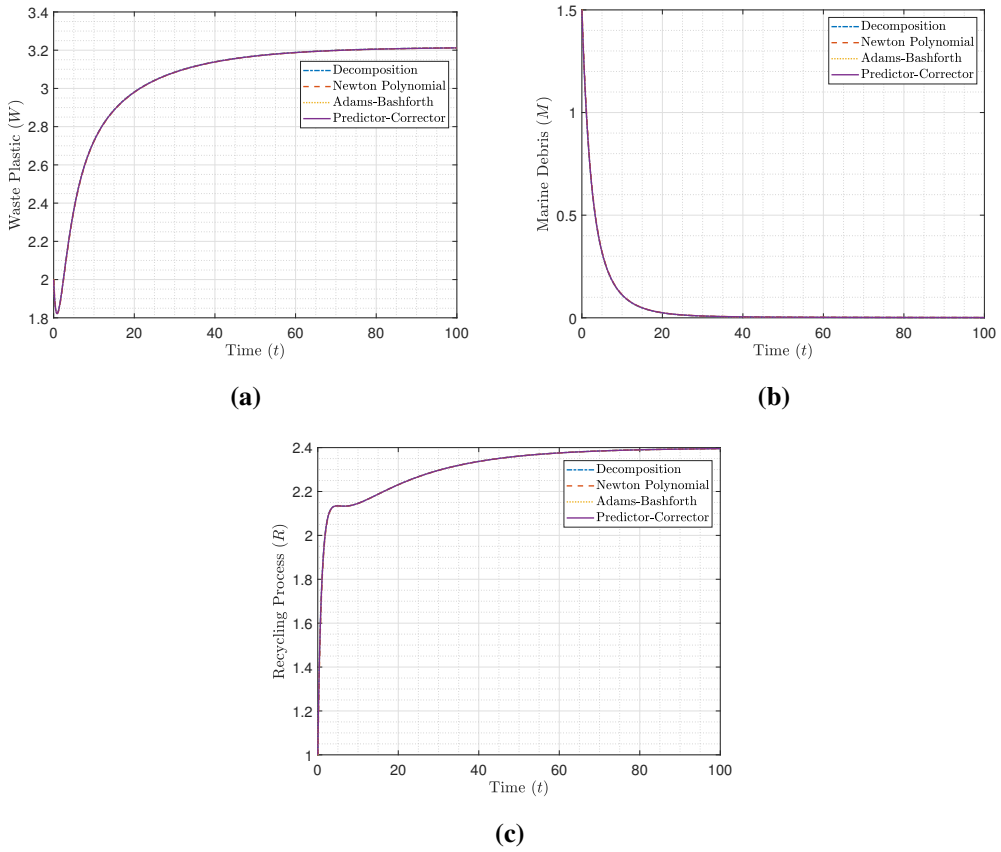

Figure 6. Conducting a comparison of the simulation results for the FFP-WPO model (2.16) using four numerical techniques.

Table 2. Numerical results for the FFP-WPO model (2.16) with $a = 0.65$, $\Lambda = 0.36$, $\mu = 0.40$, $\gamma = 0.41$, $b = \theta = 0.15$, $(W_0, M_0, R_0) = (2, 1.5, 1)$, and $\alpha = \beta = 0.99$.

Method (Day)	1	20	40	60	80	100
Waste plastic material $W(t)$						
Decomposition	1.82604	3.01710	3.16166	3.19998	3.21151	3.21532
Newton polynomial	1.82386	3.01591	3.16124	3.19976	3.21137	3.21522
Adams-Bashforth	1.82546	3.01663	3.16141	3.19981	3.21139	3.21523
Predictor-corrector	1.82553	3.01663	3.16141	3.19981	3.21139	3.21523
Marine debris $M(t)$						
Decomposition	1.03499	0.01752	0.00340	0.00191	0.00137	0.00107
Newton polynomial	1.05967	0.01782	0.00350	0.00198	0.00142	0.00111
Adams-Bashforth	1.04031	0.01770	0.00349	0.00198	0.00142	0.00111
Predictor-corrector	1.04038	0.01770	0.00349	0.00198	0.00142	0.00111
Recycling $R(t)$						
Decomposition	1.78054	2.25196	2.35490	2.38563	2.39480	2.39769
Newton polynomial	1.75212	2.25134	2.35465	2.38552	2.39474	2.39765
Adams-Bashforth	1.77453	2.25178	2.35478	2.38556	2.39475	2.39765
Predictor-corrector	1.77437	2.25177	2.35478	2.38556	2.39475	2.39765

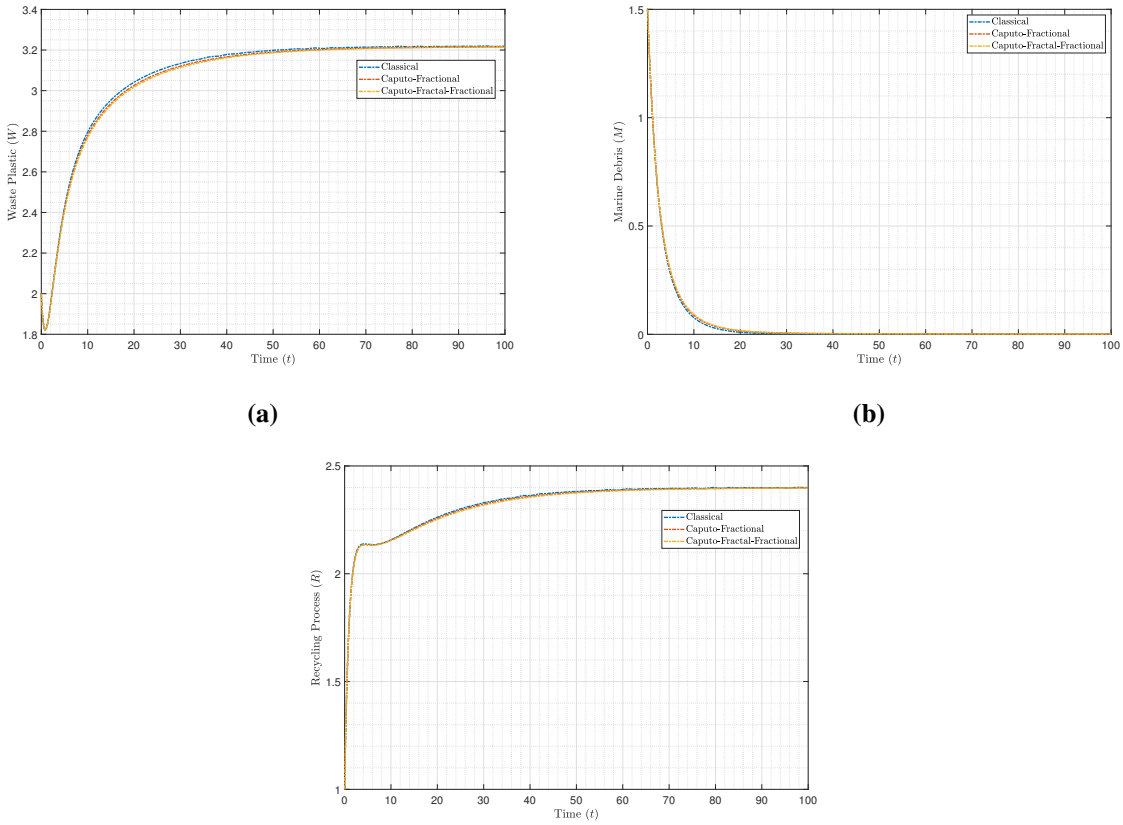

Figure 7. Comparison of the classical model, the Caputo-fractional model, and the Caputo-fractal-fractional model.

Table 3. Comparing numerical results between the classical model, the Caputo-fractional model, and the Caputo-fractal-fractional model.

Method (Day)	1	20	40	60	80	100
Waste plastic material $W(t)$						
Classical	1.82395	3.04112	3.17561	3.20932	3.21779	3.21737
Caputo-fractional	1.82605	3.02548	3.16647	3.20221	3.21246	3.21574
Caputo-fractal-fractional	1.82604	3.01710	3.16166	3.19998	3.21151	3.21532
Marine debris $M(t)$						
Classical	1.03624	0.00959	0.00026	0.0001	2.95×10^{-7}	1.04×10^{-8}
Caputo-fractional	1.03503	0.01622	0.00325	0.00186	0.00134	0.00105
Caputo-fractal-fractional	1.03499	0.01752	0.00340	0.00191	0.00137	0.00107
Recycling $R(t)$						
Classical	1.78135	2.26242	2.36594	2.39046	2.39660	2.40120
Caputo-fractional	1.78048	2.25716	2.35878	2.38747	2.39557	2.39801
Caputo-fractal-fractional	1.78054	2.25196	2.35490	2.38563	2.39480	2.39769

6.1.2. The marine debris-included equilibrium point $\mathfrak{E}_1^*$

Set $\alpha = 0.83, 0.87, 0.91, 0.95, 0.99$ and $\beta = 0.99$ with the given parameters $b = 0.75$, $a = 0.50$, $\Lambda = 0.66$, $\theta = 0.05$, $\mu = 0.40$, and $\gamma = 0.21$, and the initial conditions $(W_0, M_0, R_0) = (2, 1.5, 1)$. Then, Theorem 3.5 is satisfied. We obtain that the marine debris-included equilibrium point $\mathfrak{E}_1^* = (W_1^*, M_1^*, R_1^*) = (0.6667, 11.6, 13.2)$ is GAS, which implies that the solutions of the FFP-WPO model (2.16) should move to the marine debris-included equilibrium point $\mathfrak{E}_1^*$. In Figures 8–10, the dynamical behavior of the management of waste plastic in the ocean is shown when $P_0 = 42.4286 > 1$. In addition, Figure 8 (Figure 8a–8d) depicts the dynamical behavior of the waste plastic material $W(t)$. When α increases from 0.83 to 0.99 and β is 0.99, the process quickly increases from the start and finally converges to a stable state at $W_1^* = 0.6667$.

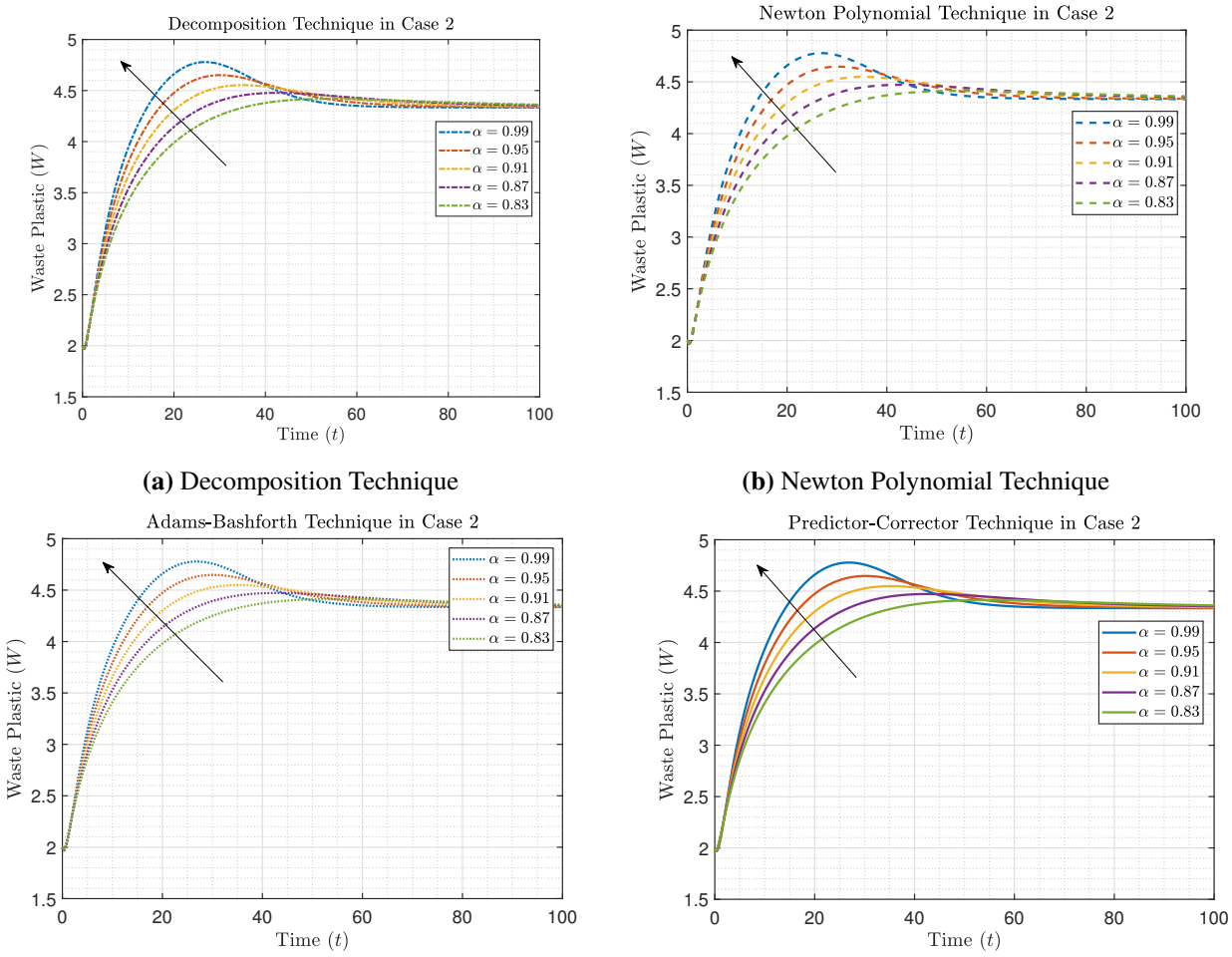

(a) Decomposition Technique

(b) Newton Polynomial Technique

(c) Adam-Bashforth Technique

(d) Predictor-Corrector Technique

Figure 8. Numerical simulations of $W(t)$ for the FFP-WPO model (2.16) using four numerical techniques.

Figure 9 (Figure 9a–9d) depicts the dynamical behavior of the marine debris $M(t)$. When α increases from 0.83 to 0.99 and β is 0.99, the process quickly decreases from the start and finally increasing converges to a stable state at $M_0^* = 11.6$.

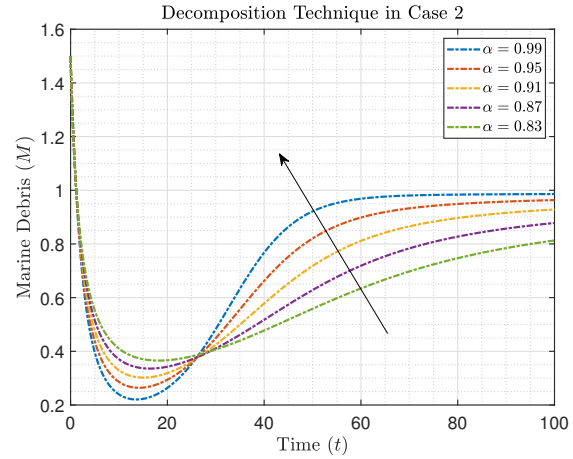

(a) Decomposition Technique

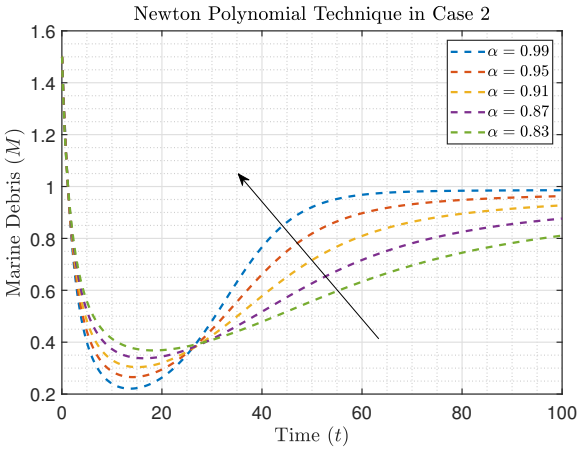

(b) Newton Polynomial Technique

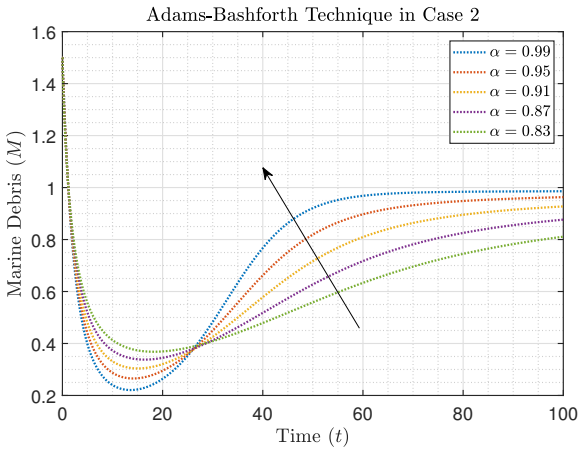

(c) Adam-Bashforth Technique

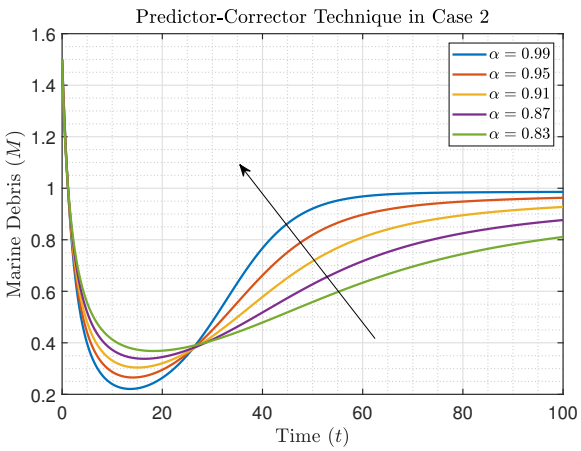

(d) Predictor-Corrector Technique

Figure 9. Numerical simulations of $M(t)$ for the FFP-WPO model (2.16) using four numerical techniques.

Figure 10 (Figure 10a–10d) depicts the dynamical behavior of the reprocessing or recycling $R(t)$. When α increases from 0.83 to 0.99 and β is 0.99, the process quickly increases from the start and finally converges to a stable state at $R_0^* = 13.2$.

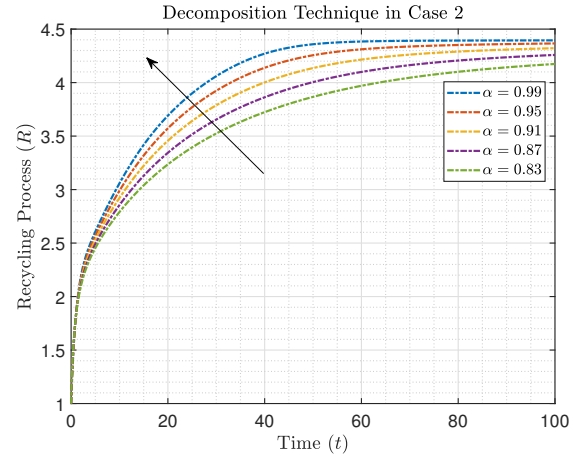

(a) Decomposition Technique

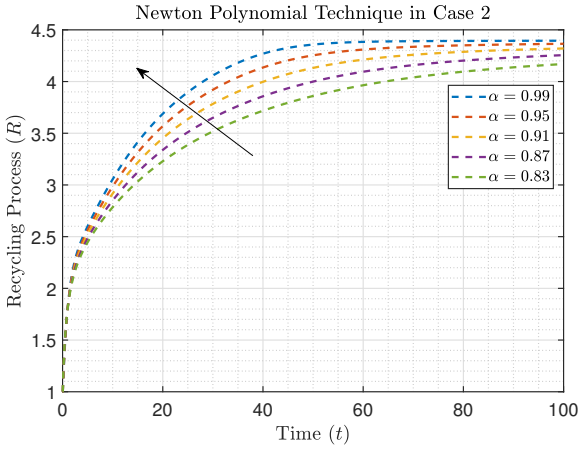

(b) Newton Polynomial Technique

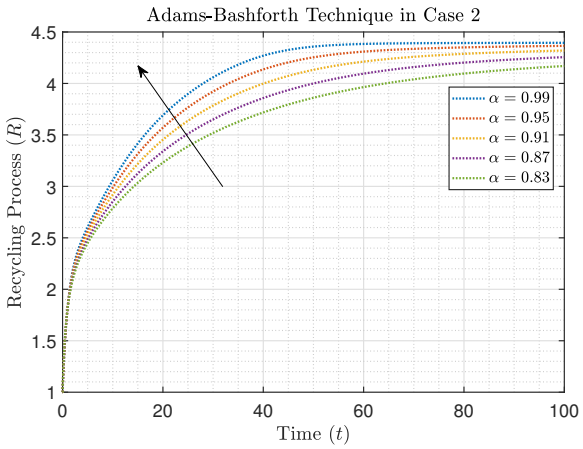

(c) Adam-Bashforth Technique

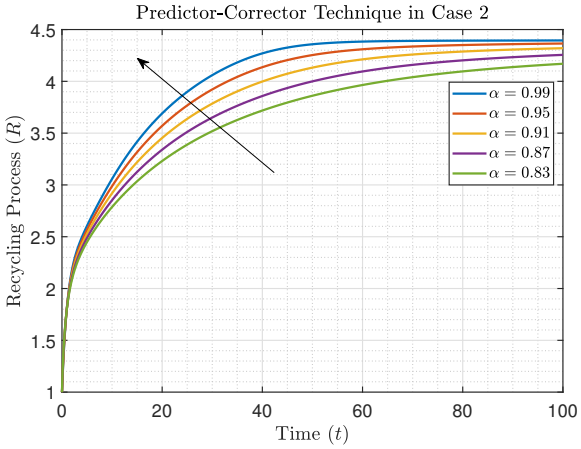

(d) Predictor-Corrector Technique

Figure 10. Numerical simulations of $R(t)$ for the FFP-WPO model (2.16) using four numerical techniques.

Using the four different numerical algorithms, Figure 11 illustrates comparisons of simulation results using four techniques for three groups: $W(t)$ (Figure 11a), $M(t)$ (Figure 11b), and $R(t)$ (Figure 11c), respectively, under $\alpha = \beta = 0.99$. To compare the results of the four numerical techniques for the three state compartments, we show some numerical results in Table 4.

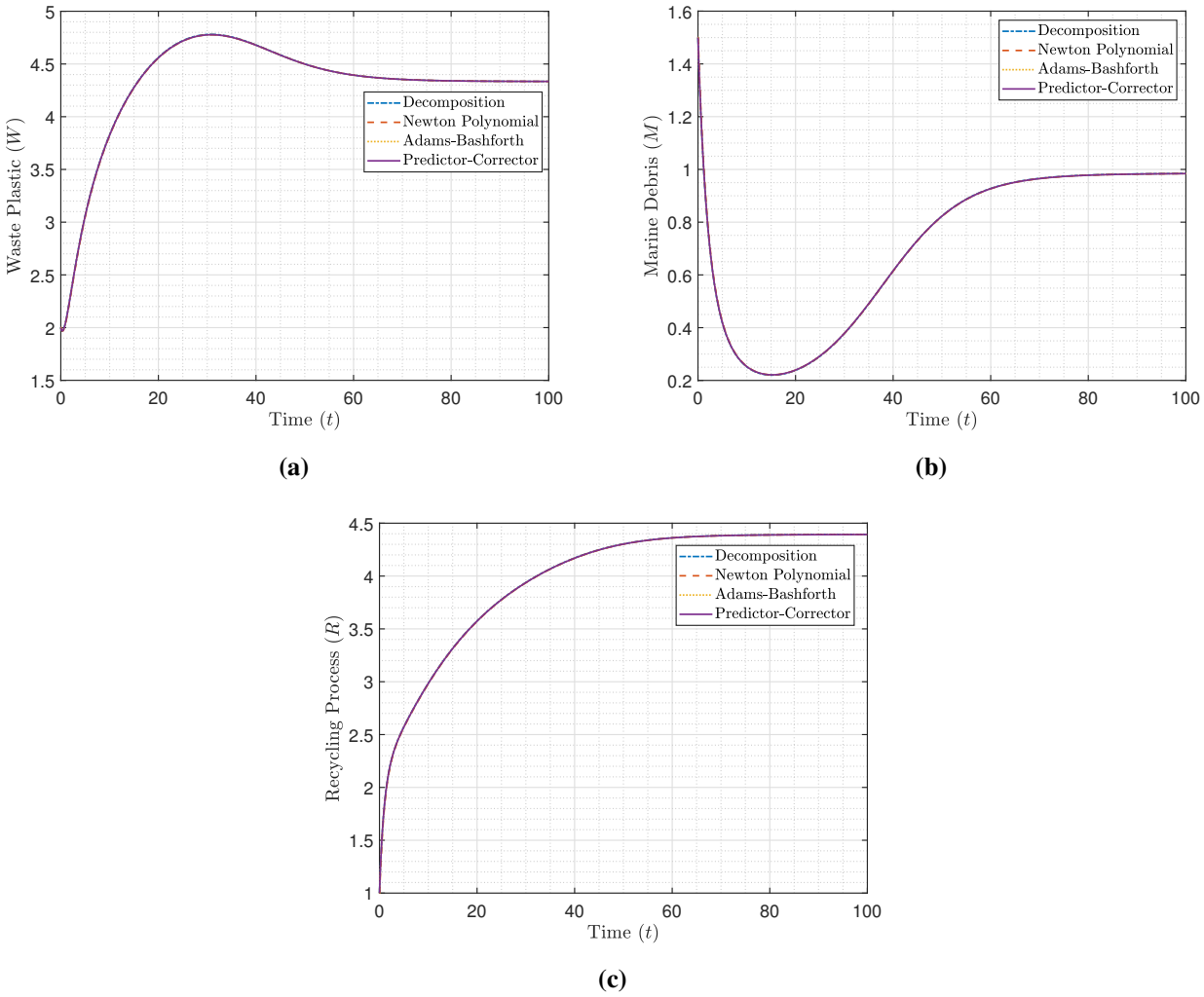

Figure 11. Conducting a comparison of the simulation results for the FFP-WPO model (2.16) using four numerical techniques.

Table 4. Numerical results for the FFP-WPO model (2.16) with $b = 0.75$, $a = 0.50$, $\Lambda = 0.66$, $\theta = 0.05$, $\mu = 0.40$, $\gamma = 0.21$, $(W_0, M_0, R_0) = (2, 1.5, 1)$, and $\alpha = \beta = 0.99$.

Method (Day)	1	20	40	60	80	100
Waste plastic material $W(t)$						
Decomposition	0.88905	0.70260	0.68241	0.67496	0.67140	0.66950
Newton polynomial	0.92173	0.70273	0.68245	0.67499	0.67142	0.66951
Adams-Bashforth	0.89588	0.70264	0.68243	0.67497	0.67141	0.66951
Predictor-corrector	0.89596	0.70264	0.68243	0.67497	0.67141	0.66951
Marine debris $M(t)$						
Decomposition	2.48739	5.83541	8.08821	9.43897	10.25836	10.75914
Newton polynomial	2.46019	5.82516	8.08129	9.43406	10.25475	10.75642
Adams-Bashforth	2.48165	5.83259	8.08574	9.43676	10.25640	10.75743
Predictor-corrector	2.48161	5.83259	8.08573	9.43676	10.25640	10.75743
Recycling $R(t)$						
Decomposition	1.71808	6.39971	9.05486	10.64860	11.61577	12.20700
Newton polynomial	1.67651	6.38762	9.04668	10.64279	11.61151	12.20378
Adams-Bashforth	1.70907	6.39636	9.05192	10.64598	11.61345	12.20497
Predictor-corrector	1.70902	6.39636	9.05192	10.64598	11.61345	12.20497

It can be observed that the graphical simulations and numerical results of these four numerical techniques are quite comparable with little difference. In addition, we also show a comparison of the results between the classical derivative, the fractional derivative, and the fractal-fractional derivative for the FFP-WPO model (2.16) in Figure 12 and Table 5.

Table 5. Comparing numerical results between the classical model, the Caputo-fractional model, and the Caputo-fractal-fractional model.

Method (Day)	1	20	40	60	80	100
Waste plastic material $W(t)$						
Classical	0.88729	0.70023	0.68106	0.67419	0.67042	0.66880
Caputo-fractional	0.88913	0.70151	0.68159	0.67436	0.67097	0.66918
Caputo-fractal-fractional	0.88905	0.70260	0.68241	0.67496	0.67140	0.66950
Marine debris $M(t)$						
Classical	2.48918	6.01042	8.35404	9.71332	10.50359	10.96254
Caputo-fractional	2.48732	5.92417	8.21720	9.56732	10.36861	10.84681
Caputo-fractal-fractional	2.48739	5.83541	8.08821	9.43897	10.25836	10.75914
Recycling $R(t)$						
Classical	1.71538	6.60659	9.36937	10.97338	11.90551	12.44737
Caputo-fractional	1.71800	6.50420	9.20699	10.80007	11.74592	12.31050
Caputo-fractal-fractional	1.71808	6.39971	9.05486	10.64860	11.61577	12.20700

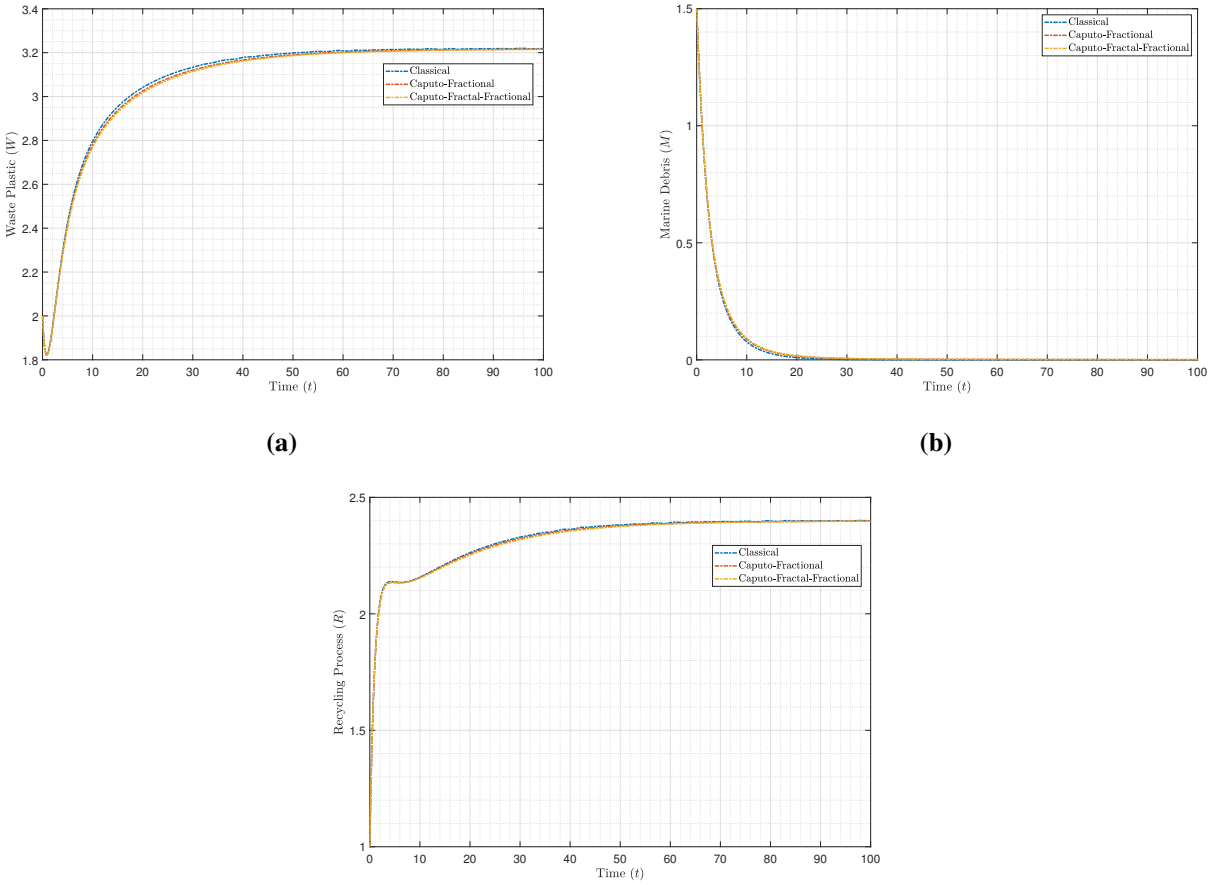

Figure 12. Comparison of the classical model, the Caputo-fractional model, and the Caputo-fractal-fractional model.

6.2. Impact of the waste rate to become marine (b) on the FFP-WPO model (2.16).

Set $\alpha = 0.95, \beta = 0.99$, and $(W_0, M_0, R_0) = (2, 1.5, 1)$ with the given parameters $\Lambda = 0.36$, $\gamma = 0.41$, $a = 0.65$, $\mu = 0.40$, $\theta = 0.15$, and $b \in [0.15, 0.60]$. Figure 13 demonstrates the influence of the parameter b on the FFP-WPO model (2.16). If the parameter b increases from 0.15 to 0.60, the stability of the equilibrium point $\mathfrak{E}_0^*$ will move to the point $\mathfrak{E}_1^*$. Furthermore, increasing the value of b by 5% from 0.15 to 0.60 (60 different values) causes the marine debris (M) quantity to shift away from zero and become positive.

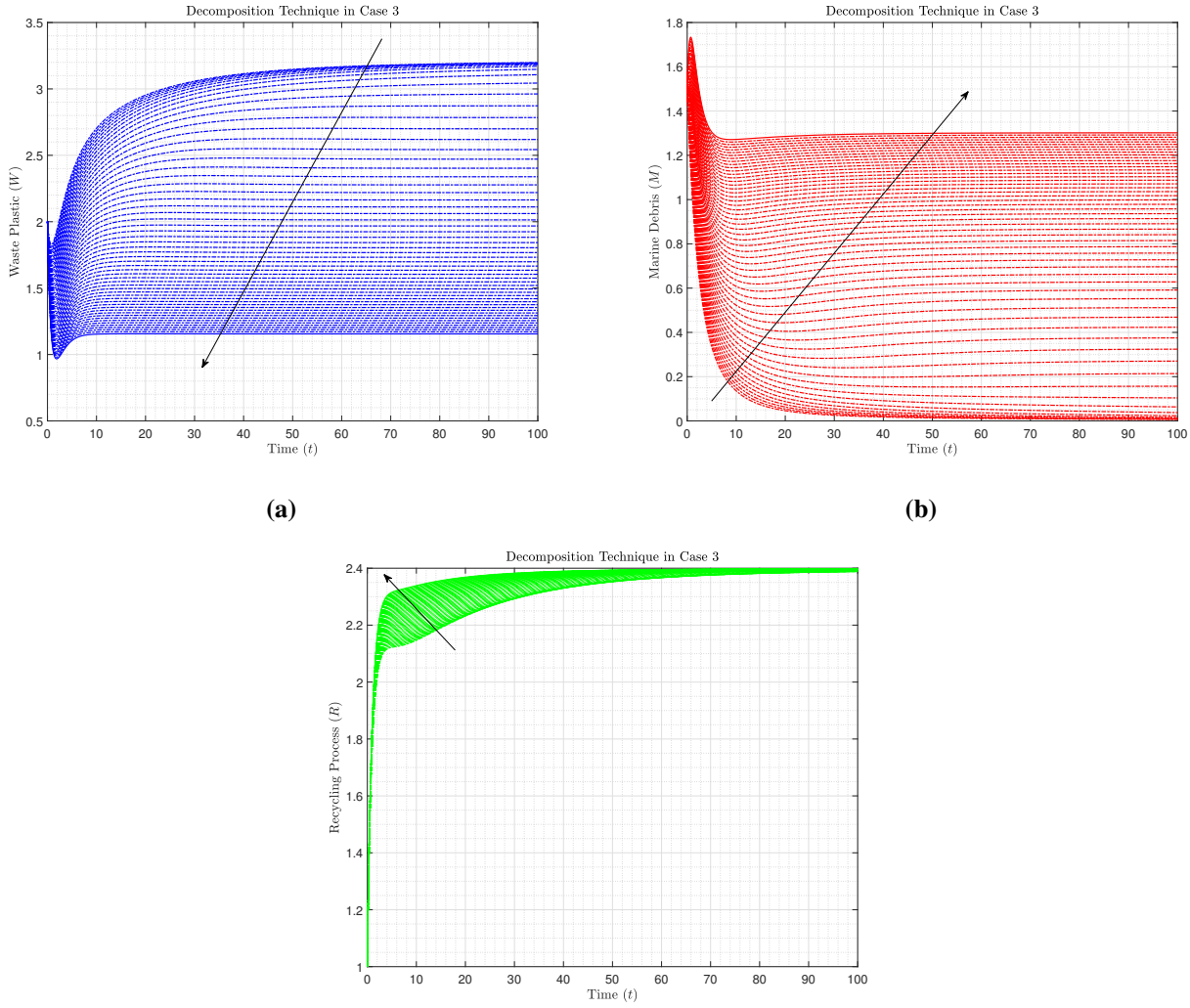

Figure 13. Numerical simulations of $W(t)$, $M(t)$, and $R(t)$ for the FFP-WPO model (2.16) with $\alpha = 0.95$, $\beta = 0.99$, $\Lambda = 0.36$, $\gamma = 0.41$, $a = 0.65$, $\mu = 0.40$, $\theta = 0.15$, and $b \in [0.15, 0.60]$.

6.3. Impact of the marine debris rate to recycle (a) on the FFP-WPO model (2.16)

Set $\alpha = 0.95, \beta = 0.99$, and $(W_0, M_0, R_0) = (2, 1.5, 1)$ with the given parameters $\Lambda = 0.36$, $\gamma = 0.41$, $b = 0.15$, $\mu = 0.40$, $\theta = 0.15$, and the parameter $a \in [0.10, 0.70]$. Figure 14 demonstrates the influence of the parameter a on the FFP-WPO model (2.16). If the parameter a increases from 0.10 to 0.70, the stability of the equilibrium point $\mathfrak{E}_1^*$ is unstable, while the equilibrium point $\mathfrak{E}_0^*$ becomes $\mathfrak{E}_1^*$ stable. Additionally, increasing the value of a by 5% from 0.10 to 0.70 (60 different values) causes the marine debris (M) quantity to approach zero.

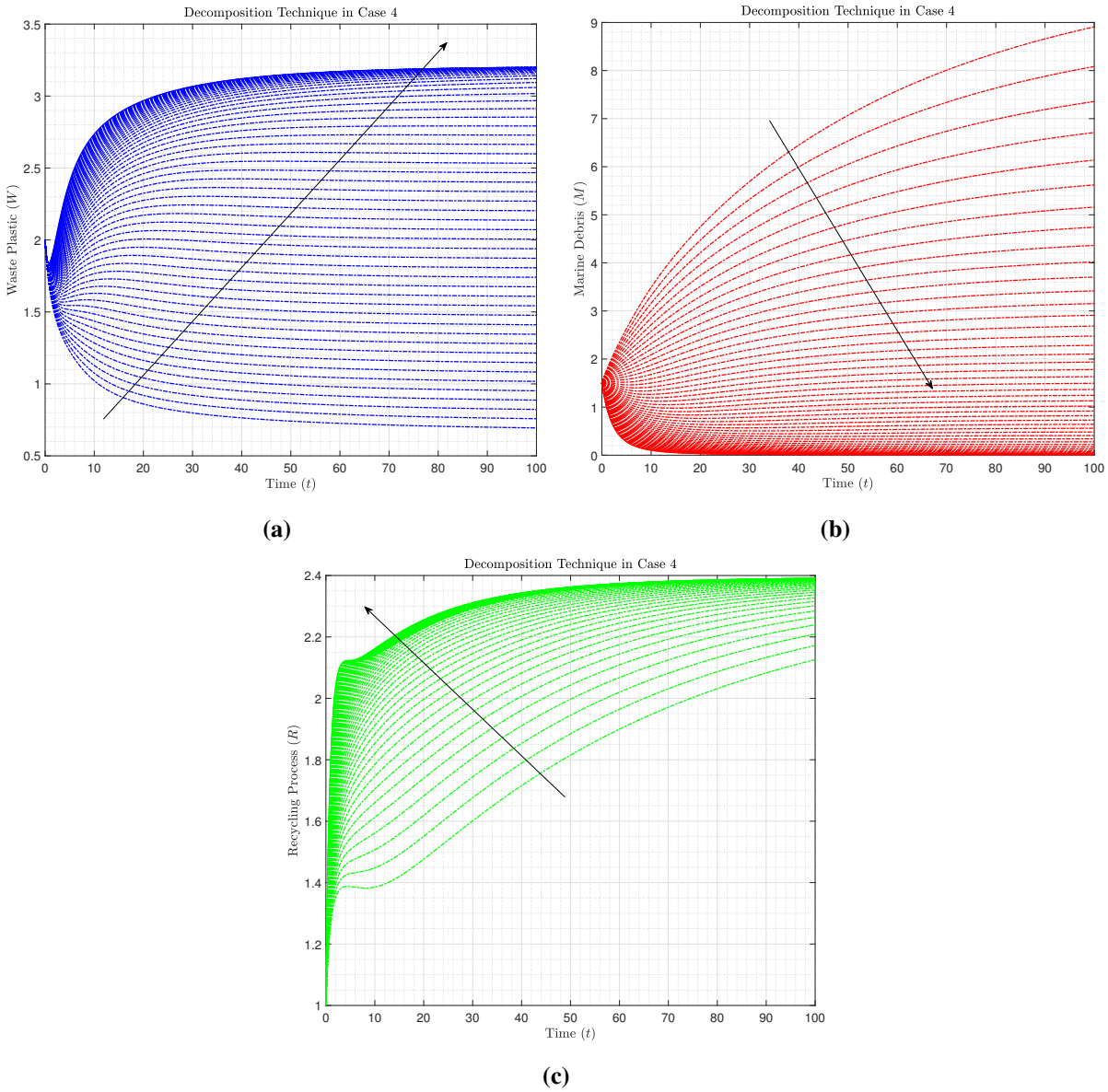

Figure 14. Numerical simulations of $W(t)$, $M(t)$, and $R(t)$ for the FFP-WPO model (2.16) with $\alpha = 0.95$, $\beta = 0.99$, $\Lambda = 0.36$, $\gamma = 0.41$, $b = 0.15$, $\mu = 0.40$, $\theta = 0.15$, and $a \in [0.10, 0.70]$.

6.4. Comparison of the simulation results on the FFP-WPO model (2.16) *with reported real data*

Next, we compare the simulation results with reported real data for 70 years from 1954 to 2024 [38] in Figure 15.

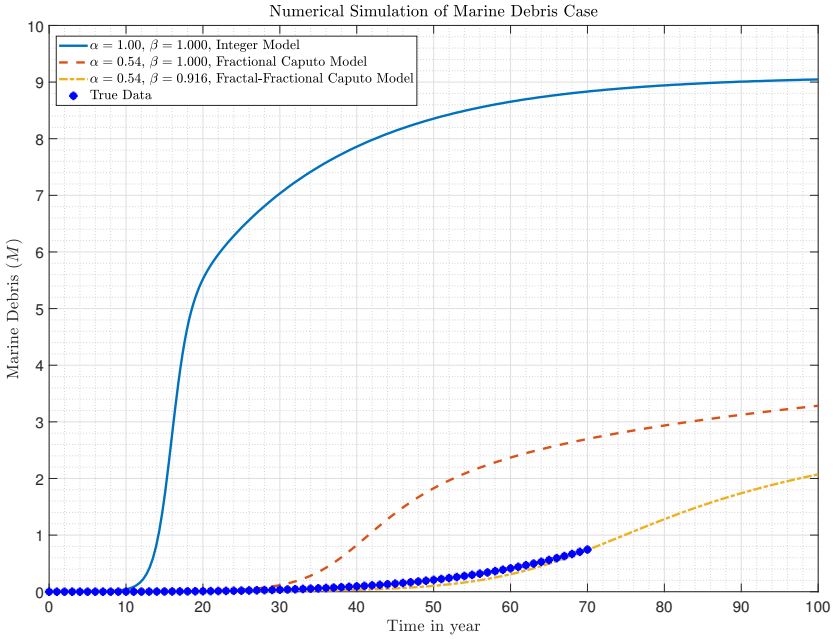

Figure 15. Comparing the integer-order, fractional-order Caputo, fractal-fractional-order Caputo, and the reported real data for the marine debris $M(t)$ of the FFP-WPO model (2.16).

Taking the given parameters $b = 0.20$, $a = 0.28$, $\Lambda = 0.66$, $\theta = 0.15$, $\mu = 0.45$, and $\gamma = 0.35$ and the initial conditions $(W_0, M_0, R_0) = (2, 0.0004, 1)$, then Theorem 3.5 is satisfied. We obtain that the marine debris-included equilibrium point $\mathfrak{E}_1^* = (W_1^*, M_1^*, R_1^*) \approx (1.40, 7.68, 4.40)$ is GAS, which implies that the solutions of the FFP-WPO model (2.16) should move to the marine debris-included equilibrium point $\mathfrak{E}_1^*$. Figure 15 displays the comparison behavior for the integer-order ($\alpha = 1.00$, $\beta = 1.000$), fractional-order Caputo ($\alpha = 0.54$, $\beta = 1.000$), fractal-fractional-order Caputo ($\alpha = 0.54$, $\beta = 0.916$), and the reported real data of the marine debris compartment. Then, the FFP-WPO model (2.16) fits the reported real data better for $\alpha = 0.54$ and $\beta = 0.916$. It is worth mentioning that fractional-order and fractal-order can have various values to give numerical results close to the reported real data. By taking use of this option, we may achieve a very close fit. Across all patients, it appears that the FFP-WPO model (2.16) is effective in predicting the majority of reported real data points, particularly those occurring early in the series.

7. Conclusions

This paper studied a developed mathematical ocean waste plastic management model through the FFP operators in the context of the power law kernel. Waste pollution of the ocean is a crisis produced by humans, endangering the ecology and aquatic life of the ocean and even disrupting rivers. The population class was categorized into three sub-classes to construct the proposed model. An approximation of the FFP derivative of $\alpha \in (0, 1)$ and $\beta \in (0, 1)$ in the Caputo sense was analyzed in Lemma 2.7. The obtained result allowed the application of methods formulating the Volterra-type Lyapunov functions in FFP systems. The positivity of the solutions for the FFP-WPO model (2.16) was demonstrated. The two equilibrium points, namely, the boundary equilibrium $\mathfrak{E}_0^*$ and the interior equilibrium $\mathfrak{E}_1^*$ points, as well as the basic reproduction number P_0, were established. If $P_0 < 1$ with

the necessary and sufficient conditions (3.6) satisfied, then the marine debris-free equilibrium point $\mathfrak{E}_0^*$ is LAS, which in the amount of marine debris is zero. The marine debris-included equilibrium point $\mathfrak{E}_1^*$ is LAS if $P_0 > 1$, and otherwise it is unstable, which corresponds to positive amounts of marine debris. By creating Lyapunov functionals, $\mathfrak{E}_0^*$ is GAS when $P_0 < 1$, while $\mathfrak{E}_1^*$ is GAS when $P_0 > 1$. Based on the aforementioned mathematical conclusions, we conclude that the memory of the FFP derivative does not affect equilibrium stability. The existence and uniqueness proofs of the FFP-WPO model (2.16) apply well-known fixed-point theorems to analyze the solution's qualitative properties. Furthermore, the stability analysis was carried out, utilizing both the UH and UHR principles and their generalization. Finally, the numerical schemes for the FFP-WPO model (2.16) were allowed to utilize four numerical methods, such as the decomposition, Adams-Bashforth, newton polynomial, and predictor-corrector methods. Based on graphical simulations, we demonstrate that the fractional order and the fractal dimension affect convergence speed and time to equilibria (Figures 3–14). A small difference in the fractional order and fractal dimension was discovered to cause a little change in the proposed model's dynamical behavior. In terms of graphical simulations and the behavior of system dynamics, the four numerical methods were essentially comparable, with just minor differences. There are notable distinctions between integer-order derivatives and fractal-fractional-order derivatives. Applying the proposed numerical scheme, we have shown various numerical results offered for different fractal and fractional orders corresponding to reported real data. The model's sensitivity was assessed by computing the normalized sensitivity index for each parameter corresponding to BRN. The sensitivity analysis results of BRN presented the parameters Λ, b, and μ relating directly to P_0, while the parameters γ, a, and θ inversely relate to P_0. The number of marine debris in the ocean $M(t)$ can be decreased (or controlled) by contemplating arrangements that create a decrease in the parameters with a direct impact or an increase in the parameters with the opposite effect on P_0. To manage marine debris, it was shown that reducing waste to marine (b) and new waste (Λ) or boosting recycling rates (a and γ) are the most effective measures. This information may be used to better develop strategies and plans for controlling marine waste in the ocean. The mathematical study of the proposed model is important because it provides a quantitative index (BRN) for understanding the asymptotic behavior of the oceanic waste recycling system. Furthermore, such an analysis determines the strength of the effect of each model parameter, as components in this cycle,causing us to act more compulsively to modify the conditions that affect the most essential elements. The fractal-fractional model was simulated against data using a different set of fractal and fractional order values, and it was discovered that altering both fractal and fractional orders provided a satisfactory match to the reported real data (Figure 15). The limitation of the proposed model is the assumption about uniform waste distribution. In the future, the FFP-WPO model (2.16) can be developed to investigate the impacts of plastic waste disposal on air pollution along with respiratory diseases. We aim to extend this model by comparing both deterministic and stochastic models. Furthermore, the research should investigate the role of effecting and reduction control techniques in waste plastic in the ocean. We anticipate that this study endeavor will benefit researchers in various fields of environmental science and improve the management of the marine trash problem.

Author contributions

Chatthai Thaiprayoon: Conceptualization, methodology, software, writing-original draft preparation, writing-review suggestions and editing, formal analysis, funding acquisition; Jutarat Kongson: Conceptualization, methodology, writing-original draft preparation, writing-review suggestions and editing, supervision; Weerawat Sudsutad: Conceptualization, methodology, software, writing-original draft preparation, writing-review suggestions and editing, formal analysis. All authors have read and approved the final version of the manuscript for publication.

Acknowledgments

C. Thaiprayoon (chatthai@go.buu.ac.th) and J. Kongson (jutarat_k@go.buu.ac.th) would like to thank Burapha University for providing bench space and support.

Use of Generative-AI tools declaration

The authors declare that they have not used Artificial Intelligence (AI) tools in the creation of this article.

Funding

This work was financially supported by (i) Burapha University (BUU), (ii) Thailand Science Research and Innovation (TSRI), and (iii) National Science Research and Innovation Fund (NSRF) (Fundamental Fund: Grant no. 100/2567).

Conflict of interest

The authors declare no conflicts of interest.

References

1. M. Al. Nuwairan, Z. Sabir, M. A. Z. Raja, A. Aldhafeeri, An advance artificial neural network scheme to examine the waste plastic management in the ocean, *AIP Adv.*, **12** (2022), 045211. https://doi.org/10.1063/5.0085737
2. S. Chaturvedi, B. P. Yadav, N. A. Siddiqui, S. K. Chaturvedi, Mathematical modelling and analysis of plastic waste pollution and its impact on the ocean surface, *J. Ocean Eng. Sci.*, **5** (2020), 136–163. https://doi.org/10.1016/j.joes.2019.09.005
3. J. A. Addor, E. N. Wiah, F. I. Alao, Mathematical model for the cyclical dynamics of plastic waste management: A two-state closed model, *J. Mater. Sci. Res. Rev.*, **5** (2022), 69–90.
4. M. Izadi, M. Parsamanesh, W. Adel, Numerical and stability investigations of the waste plastic management model in the Ocean system, *Mathematics*, **10** (2022), 4601. https://doi.org/10.3390/math10234601

5. A. A. Kilbas, H. M. Srivastava, J. J. Trujillo, Theory and applications of fractional differential equations, In: *North-Holland mathematics studies*, Elsevier, **204** (2006), 1–523.
6. U. N. Katugampola, New fractional integral unifying six existing fractional integrals, *arXiv:1612.08596*, 2016. https://doi.org/10.48550/arXiv.1612.08596
7. D. Baleanu, A. Fernandez, A. Akgúl, On a fractional operator combining proportional and classical differintegrals, *Mathematics*, **8** (2020), 360. https://doi.org/10.3390/math8030360
8. R. Hilfer, *Applications of fractional calculus in physics*, Singapore: World Scientific, 2000. https://doi.org/10.1142/3779
9. E. Uçara, N. Özdemir, A fractional model of cancer-immune system with Caputo and Caputo-Fabrizio derivatives, *Eur. Phys. J. Plus*, **136** (2021), 43. https://doi.org/10.1140/epjp/s13360-020-00966-9
10. W. Sudsutad, J. Kongson, C. Thaiprayoon, On generalized (k,ψ)-Hilfer proportional fractional operator and its applications to the higher-order Cauchy problem, *Bound. Value Probl.*, **2024** (2024), 83. https://doi.org/10.1186/s13661-024-01891-x
11. A. Atangana, Fractal-fractional differentiation and integration: Connecting fractal calculus and fractional calculus to predict complex system, *Chaos Solitons Fract.*, **102** (2017), 396–406. https://doi.org/10.1016/j.chaos.2017.04.027
12. N. Almutairi, S. Saber, On chaos control of nonlinear fractional Newton-Leipnik system via fractional Caputo-Fabrizio derivatives, *Sci. Rep.*, **13** (2023), 22726. https://doi.org/10.1038/s41598-023-49541-z
13. T. Yan, M. Alhazmi, M. Y. Youssif, A. E. Elhag, A. F. Aljohani, S. Saber, Analysis of a Lorenz model using adomian decomposition and fractal-fractional operators, *Thermal Sci.*, **28** (2024), 5001–5009. https://doi.org/10.2298/TSCI2406001Y
14. K. A. Aldwoah, M. A. Almalahi, K. Shah, M. Awadalla, R. H. Egami, Dynamics analysis of dengue fever model with harmonic mean type under fractal-fractional derivative, *AIMS Mathematics*, **9** (2024), 13894–13926. https://doi.org/10.3934/math.2024676
15. K. A. Aldwoah, M. A. Almalahi, K. Shah, Theoretical and numerical simulations on the hepatitis B virus model through a piecewise fractional order, *Fractal Fract.*, **7** (2023), 84. https://doi.org/10.3390/fractalfract7120844
16. M. Al Nuwairan, Z. Sabir, M. A. Z. Raja, M. Alnami, H. Almuslem, A stochastic study of the fractional order model of waste plastic in oceans, *Comput. Mater. Continua*, **73** (2022), 4441–4454. https://doi.org/10.32604/cmc.2022.029432
17. H. Joshi, M. Yavuz, N. Özdemir, Analysis of novel fractional order plastic waste model and its effects on air pollution with treatment mechanism, *J. Appl. Anal. Comput.*, **14** (2024), 3078–3098. https://doi.org/10.11948/20230453
18. P. Priya, A. Sabarmathi, Optimal control on ABC fractal fractional order model of micro-plastic pollution in soil and its effect on the nutrient cycle, *J. Comput. Appl. Math.*, **450** (2024), 115997. https://doi.org/10.1016/j.cam.2024.115997

19. M. Parsamanesh, M. Izadi, Global stability and bifurcations in a mathematical model for the waste plastic management in the ocean, *Sci. Rep.*, **14** (2024), 20328. https://doi.org/10.1038/s41598-024-71182-z

20. S. M. Ulam, *A collection of mathematical problems*, New York: Interscience Publishers, Inc., 1960.

21. D. H. Hyers, On the stability of the linear functional equation, *Proc. Natl. Acad. Sci. U.S.A.*, **27** (1941), 222–224. https://doi.org/10.1073/pnas.27.4.222

22. T. M. Rassias, On the stability of the linear mappings in Banach spaces, *Proc. Amer. Math. Soc.*, **72** (1978), 297–300. https://doi.org/10.2307/2042795

23. A. Atangana, S. Qureshi, Modeling attractors of chaotic dynamical systems with fractal-fractional operators, *Chaos Solitons Fract.*, **123** (2019), 320–337. https://doi.org/10.1016/j.chaos.2019.04.020

24. C. Vargas-De-Léon, Volterra-type Lyapunov functions for fractional-order epidemic systems, *Commun. Nonlinear Sci. Numer. Simul.*, **24** (2015), 75–85. http://dx.doi.org/10.1016/j.cnsns.2014.12.013

25. A. Atangana, A. Akgül, On solutions of fractal fractional differential equations, *Discrete Contin. Dyn. Syst. Ser. S*, **14** (2021), 3441–3457. https://doi.org/10.3934/dcdss.2020421

26. T. Abdeljawad, On conformable fractional calculus, *J. Comput. Appl. Math.*, **279** (2015), 57–66. https://doi.org/10.1016/j.cam.2014.10.016

27. P. van den Driessche, J. Watmough, Reproduction numbers and sub-threshold endemic equilibria for compartmental models of disease transmission, *Math. Biosci.*, **180** (2002), 29–48. https://doi.org/10.1016/S0025-5564(02)00108-6

28. D. Matignon, Stability results for fractional differential equations with applications to control processing, *Comput. Eng. Syst. Appl.*, **2** (1996), 963–968.

29. M. Y. Li, H. L. Smith, L. Wang, Global dynamics of an SEIR epidemic model with vertical transmission, *SIAM J. Appl. Math.*, **62** (2001), 58–69. https://doi.org/10.1137/S0036139999359860

30. P. van den Driessche, Reproduction numbers of infectious disease models, *Infect. Dis. Model.*, **2** (2017), 288–303. http://dx.doi.org/10.1016/j.idm.2017.06.002

31. A. Granas, J. Dugundji, Fixed point theory, In: *Springer monographs in mathematics*, New York: Springer, 2003. https://doi.org/10.1007/978-0-387-21593-8

32. R. Almeida, A. B. Malinowska, T. Odzijewicz, Fractional differential equations with dependence on the Caputo-Katugampola derivative, *J. Comput. Nonlinear Dynam.*, **11** (2016), 061017. https://doi.org/10.1115/1.4034432

33. W. Sudsutad, C. Thaiprayoon, A. Aphithana, J. Kongson, W. Sae-Dan, Qualitative results and numerical approximations of the (k,ψ)-Caputo proportional fractional differential equations and applications to blood alcohol levels model, *AIMS Mathematics*, **9** (2024), 34013–34041. https://doi.org/10.3934/math.20241622

34. W. Sudsutad, C. Thaiprayoon, J. Kongson, W. Sae-Dan, A mathematical model for fractal-fractional monkeypox disease and its application to real data, *AIMS Mathematics*, **9** (2024), 8516–8563. https://doi.org/10.3934/math.2024414

35. A. Atangana, S. I. Araz, *New numerical scheme with Newton polynomial—Theory, methods, and applications*, Academic Press, 2021. https://doi.org/10.1016/C2020-0-02711-8

36. Z. Odibat, D. Baleanu, Numerical simulation of initial value problems with generalized Caputo-type fractional derivatives, *Appl. Numer. Math.*, **156** (2021), 94–105. https://doi.org/10.1016/j.apnum.2020.04.015

37. J. Kongson, C. Thaiprayoon, A. Neamvonk, J. Alzabut, W. Sudsutad, Investigation of fractal-fractional HIV infection by evaluating the drug therapy effect in the Atangana-Baleanu sense, *Math. Biosci. Eng.*, **19** (2022), 10762–10808. https://doi.org/10.3934/mbe.2022504

38. L. Lebreton, M. Egger, B. Slat, A global mass budget for positively buoyant macroplastic debris in the ocean, *Sci. Rep.*, **9** (2019), 12922. https://doi.org/10.1038/s41598-019-49413-5

AIMS Press